Computers and Mathematics with Applications 116 (2022) 212–228

Contents lists available at ScienceDirect

Computers and Mathematics with Applications

www.elsevier.com/locate/camwa

A C^1 virtual element method for the stationary quasi-geostrophic equations of the ocean

David Mora [a,b,*], Alberth Silgado [a]

[a] GIMNAP, Departamento de Matemática, Universidad del Bío-Bío, Concepción, Chile
[b] CI2MA, Universidad de Concepción, Concepción, Chile

ARTICLE INFO

Keywords:
Virtual element method
Quasi-geostrophic equations
Stream-function formulation
Error estimates

ABSTRACT

In this present paper, we propose and analyze a C^1-conforming virtual element method to solve the so-called one-layer stationary quasi-geostrophic equations (QGE) with applications in the large scale wind-driven ocean circulation, formulated in terms of the stream-function. This problem corresponds to a nonlinear fourth order partial differential equation. The C^1 virtual space and the discrete scheme are built in a straightforward way due to the flexibility of the virtual approach. Under the assumption of small data, we prove well-posedness of the discrete problem by using a fixed-point strategy and under standard assumptions on the computational domain, we establish error estimates in H^2-norm for the stream-function. Finally, we report four numerical experiments that illustrate the behavior of the proposed scheme and confirm our theoretical results on different families of polygonal meshes.

1. Introduction

The quasi-geostrophic equations (QGE) is one of the popular mathematical models employed for understanding the behavior of the large scale wind-driven ocean circulation [40,45,46]. Due to their important role in the climate system, there has been a growing interest in recent years towards developing efficient numerical schemes to solve such equations. We are going to consider the so-called one-layer QGE (also called as the barotropic vorticity equation), where the flow is assumed to be homogeneous in the vertical direction. Thus, stratification effects are ignored in this model and a bi-dimensional nonlinear fourth order partial differential equation, in terms of the stream-function variable, can be written. Despite the simplifications, the model preserves many of the essential features of the underlying large scale ocean flows. Further details related to the derivation of these equations can be found in [39,41]. On the other hand, we note that the QGE equations can be seen as an extension of the stream-function formulation of the Navier-Stokes equations (NSE).

Different finite element discretizations have been developed recently for these equations. For instance, in [27] is presented a conforming finite element based on the Argyris element, optimal error estimates are obtained and several numerical experiments are reported. In [36] the authors present a B-spline based conforming finite element method to approximate the stream-function, also several numerical simulations are performed. Error estimates for this method are presented in [33] and a posteriori error analysis has been recently analyzed in [2]. In [35], is presented a non-conforming C^0-discontinuous Galerkin method, the authors introduced the new variational form of the method and they established consistency and error estimates. In addition, the quasi-geostrophic equations have been solved by using different finite element methods in terms of the stream-function and vorticity variables in the following references [16,26,42,43]. Moreover, finite element methods for the Navier-Stokes equations in stream-function formulation have been presented in [17,18,24,25,30].

It is well known that conforming finite element spaces of H^2 are of complex implementation and contain high order polynomials (see [21]). In order to overcome this drawback, in this work, we extend the virtual element approach proposed in [4] for the numerical solution of the QGE equations in stream-function formulation, which can be applied to general polygonal meshes and is simple in terms of degrees of freedom and coding aspects. In fact, it has been shown that the VEM permits to easily implement highly regular discrete spaces on general polygonal meshes. For instance, global discrete virtual spaces of H^2 to solve fourth order PDEs have been presented in [4,13,20] (see also [9,44]). Moreover, it has been recently presented in [6] a C^1 virtual element method on polyhedral meshes. The numerical solution by virtual elements of incompressible flow

* Corresponding author.
E-mail addresses: dmora@ubiobio.cl (D. Mora), alberth.silgado1701@alumnos.ubiobio.cl (A. Silgado).

https://doi.org/10.1016/j.camwa.2021.05.022

Available online 8 June 2021

problems (Stokes, Brinkman, Stokes–Darcy and Navier-Stokes equations) have been recently developed in the following references [3,7,8,10,14,15,19,23,29,37,38,47,48].

According to the above discussion, in the present contribution, we are interested in keeping on exploring the flexibility of the VEM to solve the QGE equations with applications in oceanic circulation. More precisely, we propose and analyze a conforming C^1 virtual element discretization of lowest order, which is based on the virtual space introduced in [4], to solve the quasi-geostrophic equations in stream-function formulation. We observe that the functions, in the virtual space, have continuous trace and the trace of the gradient is also continuous; thus, the method delivers a conforming solution. We write a discrete formulation by using projector operators to construct discrete version of the local bilinear forms and trilinear form along with a discrete load term. We prove well-posedness of the discrete virtual formulation by using the Banach fixed-point Theorem and assuming that the data is in a certain sense small enough. We write error estimates in H^2-norm for the stream-function under rather mild assumptions on the polygonal meshes. Finally, we point out that, the present analysis for the stationary QGE equations constitutes a stepping-stone towards other related problems. For instance, two-layer quasi-geostrophic model [42] or time dependent QGE equations [28].

Outline The paper is organized as follows: In Section 2, we recall the quasi-geostrophic equations in terms of the stream-function and introduce the corresponding variational formulation for the system. In Section 3, we present the C^1-virtual element discretization of the variational formulation. Under the assumption of small data, we prove the existence and uniqueness of the discrete problem by using the Banach fixed-point Theorem. In Section 4, we establish error estimates for the stream-function. Four numerical tests that allow us to assess the convergence properties of the method and to check whether the experimental rates of convergence agree with the theoretical ones are reported in Section 5.

Notations Throughout the paper, we will follow the usual notation for Sobolev spaces and norms [1]. We will denote by $\Omega \subset \mathbb{R}^2$ a polygonal bounded simply connected domain and by $\boldsymbol{n} = (n_i)_{i=1,2}$ the outward unit normal vector to the boundary $\partial\Omega$. For $\mathcal{D}$ an open bounded domain, the $L^2(\mathcal{D})$ inner-product will be denoted by $(\cdot,\cdot)_{0,\mathcal{D}}$. In addition, we will denote by $\mathcal{P}_\ell(\mathcal{D})$ the space of polynomials of degree up to $\ell \in \mathbb{N}$ defined on $\mathcal{D}$. Moreover, c and C, with or without subscripts, hats or tildes, will represent a generic positive constant independent of the mesh parameter h, assuming different values in different occurrences. In addition, for any vector field $\boldsymbol{v} = (v_i)_{i=1,2}$ and any scalar field θ we recall the differential operators:

$$\operatorname{rot} \boldsymbol{v} := \partial_x v_2 - \partial_y v_1, \quad \nabla\theta := \begin{pmatrix} \partial_x\theta \\ \partial_y\theta \end{pmatrix}, \quad \mathbf{curl}\,\theta := \begin{pmatrix} \partial_y\theta \\ -\partial_x\theta \end{pmatrix}.$$

2. The model problem

Let $\Omega \subset \mathbb{R}^2$ be a polygonal bounded simply connected domain with boundary $\Gamma := \partial\Omega$. We consider the steady one-layer quasi-geostrophic equations in stream-function formulation (for further details, see for instance [27]):

$$\begin{aligned} \mathrm{Re}^{-1}\Delta^2\psi - \mathbf{curl}\,\psi\cdot\nabla(\Delta\psi) - \mathrm{Ro}^{-1}\partial_x\psi = \mathrm{Ro}^{-1} f \qquad & \text{in } \Omega, \\ \psi = \partial_n\psi = 0 \qquad & \text{on } \Gamma, \end{aligned} \tag{2.1}$$

where ψ is the stream-function of the velocity field $\boldsymbol{u}$, i.e., $\boldsymbol{u} = \mathbf{curl}\,\psi$, ∂_n denotes the normal derivative and f is the source term. The constants Re and Ro denote the Reynolds and Rossby numbers, respectively. These parameters are defined by (see [27,31,32]):

$$\mathrm{Re} := \frac{U\,L}{A_H} \qquad \text{and} \qquad \mathrm{Ro} := \frac{U}{\beta\,L^2},$$

where the coefficient β is the coefficient multiplying the y-coordinate in the β-plane (see [46]), L is the characteristic length scale, U is the characteristic velocity scale and A_H is the eddy viscosity parametrization.

In order to write a weak formulation of problem (2.1), we consider the following space:

$$X := \left\{\phi \in H^2(\Omega) : \phi = \partial_n\phi = 0 \quad \text{on} \quad \Gamma\right\}.$$

We endow the space X with the following norm

$$\|\phi\|_X := |\phi|_{2,\Omega} \qquad \forall\phi \in X.$$

Now, we multiply the corresponding equation by a test function $\phi \in X$, integrate twice by parts in Ω and using the boundary conditions, we obtain the following variational problem: find $\psi \in X$ such that:

$$\mathrm{Re}^{-1}A(\psi,\phi) + B(\psi;\psi,\phi) - \mathrm{Ro}^{-1}C(\psi,\phi) = \mathrm{Ro}^{-1}F(\phi) \qquad \forall\phi \in X, \tag{2.2}$$

where $A, C : X \times X \to \mathbb{R}$ are bilinear forms, $B : X \times X \times X \to \mathbb{R}$ is a trilinear form and $F : X \to \mathbb{R}$ is a linear functional, defined as follows:

$$A(\psi,\phi) := \int_\Omega \mathrm{D}^2\psi : \mathrm{D}^2\phi \qquad \forall\psi,\phi \in X, \tag{2.3}$$

$$B(\zeta;\psi,\phi) := \int_\Omega \Delta\zeta\,\mathbf{curl}\,\psi\cdot\nabla\phi \qquad \forall\zeta,\psi,\phi \in X, \tag{2.4}$$

$$C(\psi,\phi) := \int_\Omega \partial_x\psi\,\phi \qquad \forall\psi,\phi \in X, \tag{2.5}$$

$$F(\phi) := \int_\Omega f\,\phi \qquad \forall\phi \in X, \tag{2.6}$$

where we denote by “:” the usual scalar product of 2×2-matrices and by $\mathrm{D}^2\phi$ the Hessian matrix of ϕ.

Using integration by part and the boundary conditions, it is easy to see that bilinear form $C(\cdot,\cdot)$ defined in (2.5) satisfies,

$$C(\psi,\phi) = -C(\phi,\psi) \qquad \forall \psi,\phi \in X.$$

Now, we introduce the following bilinear form $C_{\text{skew}} : X\times X \to \mathbb{R}$:

$$C_{\text{skew}}(\psi,\phi) := \frac{1}{2}C(\psi,\phi) - \frac{1}{2}C(\phi,\psi) = \frac{1}{2}\int_\Omega \partial_x\psi\,\phi - \frac{1}{2}\int_\Omega \partial_x\phi\,\psi \qquad \forall \psi,\phi \in X. \tag{2.7}$$

Clearly

$$C_{\text{skew}}(\psi,\phi) = C(\psi,\phi) \qquad \forall \psi,\phi \in X.$$

Thus, according to the above equality, we rewrite the variational problem (2.2) in the following equivalent weak form: find $\psi \in X$ such that:

$$\mathrm{Re}^{-1}A(\psi,\phi) + B(\psi;\psi,\phi) - \mathrm{Ro}^{-1}C_{\text{skew}}(\psi,\phi) = \mathrm{Ro}^{-1}F(\phi) \qquad \forall \phi \in X. \tag{2.8}$$

Remark 2.1. We observe that our VEM discretization will be based on the above weak form. In particular, to discretize the skew-symmetric bilinear form $C_{\text{skew}}(\cdot,\cdot)$ (cf. (2.7)), we construct a simple discrete form that preserves the skew-symmetric property at discrete level, which makes the analysis of the method simpler. For instance, we observe that the analysis of existence and uniqueness of the discrete problem and the convergence analysis of the method (see Sections 3.3 and 4, respectively) are facilitated using the skew-symmetric bilinear form.

The following lemma establishes some properties for the forms (2.3), (2.4), (2.6) and (2.7), these properties will play an important role in the forthcoming sections.

Lemma 2.1. *There exist positive constants $\widehat{C}_B, \widehat{C}_1$ such that*

$$|A(\psi,\phi)| \le \|\psi\|_X\|\phi\|_X \qquad \forall \psi,\phi \in X, \tag{2.9}$$

$$A(\phi,\phi) \ge \|\phi\|_X^2 \qquad \forall \phi \in X, \tag{2.10}$$

$$|B(\zeta;\psi,\phi)| \le \widehat{C}_B\,\|\zeta\|_X\|\psi\|_X\|\phi\|_X \qquad \forall \zeta,\psi,\phi \in X, \tag{2.11}$$

$$B(\zeta;\psi,\phi) = -B(\zeta;\phi,\psi) \qquad \forall \zeta,\psi,\phi \in X, \tag{2.12}$$

$$B(\zeta;\phi,\phi) = 0 \qquad \forall \zeta,\phi \in X, \tag{2.13}$$

$$|C_{\text{skew}}(\psi,\phi)| \le \widehat{C}_1\,\|\psi\|_X\|\phi\|_X \qquad \forall \psi,\phi \in X, \tag{2.14}$$

$$C_{\text{skew}}(\phi,\phi) = 0 \qquad \forall \phi \in X, \tag{2.15}$$

$$|F(\phi)| \le \|f\|_{-2,\Omega}\|\phi\|_X \qquad \forall \phi \in X. \tag{2.16}$$

Proof. The proof follows standard arguments. □

In order to prove the well posedness of problem (2.8), we will employ a fixed-point strategy. Indeed, given $\zeta \in X$, we define the following operator

$$T : X \longrightarrow X$$
$$\zeta \longmapsto T(\zeta) = \varphi,$$

where φ is the solution of the following linear problem: find $\varphi \in X$ such that

$$\mathcal{Q}_\zeta(\varphi,\phi) = \mathrm{Ro}^{-1}F(\phi) \qquad \forall \phi \in X, \tag{2.17}$$

where the bilinear form $\mathcal{Q}_\zeta(\cdot,\cdot)$ is given by

$$\mathcal{Q}_\zeta(\varphi,\phi) := \mathrm{Re}^{-1}A(\varphi,\phi) + B(\zeta;\varphi,\phi) - \mathrm{Ro}^{-1}C_{\text{skew}}(\varphi,\phi).$$

We note that $\psi \in X$ is a solution of problem (2.8) if and only if $T(\psi) = \psi$. Thus, to prove well posedness of (2.8), we will prove that T has a unique fixed point by means of the classical Banach fixed-point Theorem (see [22, Theorem 3.7-1]).

The following lemma establishes that the bilinear form $\mathcal{Q}_\zeta(\cdot,\cdot)$ is bounded and elliptic. Thus, operator T is well defined.

Lemma 2.2. *There exists a positive constant C_Q such that*

$$\mathcal{Q}_\zeta(\varphi,\phi) \le C_Q\|\varphi\|_X\|\phi\|_X \qquad \forall \varphi,\phi \in X,$$

and

$$\mathcal{Q}_\zeta(\phi,\phi) \ge \mathrm{Re}^{-1}\|\phi\|_X^2 \qquad \forall \phi \in X.$$

Proof. The result follows from Lemma 2.1. □

By a direct application of Lax-Milgram Theorem we conclude that problem (2.17) has a unique solution. In addition, from the definition of the continuous problem (cf. (2.17)), (2.13), (2.15) and (2.16), the following continuous dependence holds

$$\|\varphi\|_X \leq \mathrm{Ro}^{-1}\mathrm{Re}\,\|f\|_{-2,\Omega}.$$

Thus, operator T is well defined.

In what follows, we will prove that T is a contraction mapping. Let $\delta := \mathrm{Ro}^{-1}\mathrm{Re}\|f\|_{-2,\Omega}$, then we consider the following bounded set

$$\mathcal{N} := \{\phi \in X : \|\phi\|_X \leq \delta\},$$

and using the previous lemma, we have that $T(\mathcal{N}) \subseteq \mathcal{N}$.

The following lemma establishes that T is a contraction mapping and hence, according to the Banach fixed-point Theorem, it has a unique fixed point in $\mathcal{N}$ (see [22, Theorem 3.7-1]).

Lemma 2.3. *Assume that*

$$\widehat{C}_B\mathrm{Ro}^{-1}\mathrm{Re}^2\|f\|_{-2,\Omega} < 1. \tag{2.18}$$

Then, T is a contraction mapping in $\mathcal{N}$.

Proof. Let $\zeta_1, \psi_1, \zeta_2, \psi_2 \in \mathcal{N}$, such that

$$T(\zeta_1) = \psi_1 \qquad \text{and} \qquad T(\zeta_2) = \psi_2,$$

then from the definition of the operator $T(\cdot)$, we have

$$\mathrm{Re}^{-1}A(\psi_1,\phi) + B(\zeta_1;\psi_1,\phi) - \mathrm{Ro}^{-1}C_{\mathrm{skew}}(\psi_1,\phi) = \mathrm{Ro}^{-1}F(\phi) \qquad \forall \phi \in X, \tag{2.19}$$

$$\mathrm{Re}^{-1}A(\psi_2,\phi) + B(\zeta_2;\psi_2,\phi) - \mathrm{Ro}^{-1}C_{\mathrm{skew}}(\psi_2,\phi) = \mathrm{Ro}^{-1}F(\phi) \qquad \forall \phi \in X. \tag{2.20}$$

Subtracting (2.20) from (2.19), we get

$$\mathrm{Re}^{-1}A(\psi_1-\psi_2,\phi) + [B(\zeta_1;\psi_1,\phi) - B(\zeta_2;\psi_2,\phi)] - \mathrm{Ro}^{-1}C_{\mathrm{skew}}(\psi_1-\psi_2,\phi) = 0 \quad \forall \phi \in X.$$

Now, taking $\phi := \psi_1 - \psi_2$ in the above equation, we have that $C_{\mathrm{skew}}(\cdot,\cdot)$ vanishes (cf. (2.15)). Thus, we get

$$\mathrm{Re}^{-1}A(\psi_1-\psi_2,\psi_1-\psi_2) + B(\zeta_1;\psi_1,\psi_1-\psi_2) - B(\zeta_2;\psi_2,\psi_1-\psi_2) = 0.$$

Then, by adding and subtracting ψ_2 in the second term, we have

$$\begin{aligned}
0 &= \mathrm{Re}^{-1}A(\psi_1-\psi_2,\psi_1-\psi_2) + B(\zeta_1;\psi_1-\psi_2,\psi_1-\psi_2) + B(\zeta_1;\psi_2,\psi_1-\psi_2) - B(\zeta_2;\psi_2,\psi_1-\psi_2)\\
&= \mathrm{Re}^{-1}A(\psi_1-\psi_2,\psi_1-\psi_2) + B(\zeta_1;\psi_2,\psi_1-\psi_2) - B(\zeta_2;\psi_2,\psi_1-\psi_2)\\
&= \mathrm{Re}^{-1}A(\psi_1-\psi_2,\psi_1-\psi_2) + B(\zeta_1-\zeta_2;\psi_2,\psi_1-\psi_2),
\end{aligned}$$

where we have used (2.13). Therefore

$$\mathrm{Re}^{-1}A(\psi_1-\psi_2,\psi_1-\psi_2) = -B(\zeta_1-\zeta_2;\psi_2,\psi_1-\psi_2),$$

by using (2.10), (2.11) and the Cauchy-Schwarz inequality, we obtain

$$\mathrm{Re}^{-1}\|\psi_1-\psi_2\|_X^2 \leq \widehat{C}_B\|\psi_2\|_X\|\zeta_1-\zeta_2\|_X\|\psi_1-\psi_2\|_X,$$

then, using the fact that $\psi_2 \in \mathcal{N}$, we get

$$\|\psi_1-\psi_2\|_X \leq \widehat{C}_B\mathrm{Re}\left(\mathrm{Ro}^{-1}\mathrm{Re}\|f\|_{-2,\Omega}\right)\|\zeta_1-\zeta_2\|_X = \widehat{C}_B\mathrm{Ro}^{-1}\mathrm{Re}^2\|f\|_{-2,\Omega}\|\zeta_1-\zeta_2\|_X.$$

Therefore, according to assumption (2.18), we obtain that T is a contraction mapping, which concludes the proof. □

The following result follows from Lemma 2.3 and the Banach fixed-point Theorem.

Theorem 2.1. *If*

$$\lambda := \widehat{C}_B\,\mathrm{Re}^2\mathrm{Ro}^{-1}\|f\|_{-2,\Omega} < 1,$$

there exists a unique $\psi \in \mathcal{N}$ solution to problem (2.8), which satisfies the following continuous dependence

$$\|\psi\|_X \leq \mathrm{Re}\,\mathrm{Ro}^{-1}\|f\|_{-2,\Omega}.$$

In what follows, we will assume that the source term satisfies $f \in L^2(\Omega)$. Now, we state an additional regularity result for the solution of problem (2.8). The proof of this result can be found in [34, Lemma 2.3] (see also [11]).

Theorem 2.2. *Let $\psi \in \mathcal{N}$ be the unique solution of problem (2.8). Then, there exist $s \in (1/2, 1]$ and $\widetilde{C} > 0$ such that $\psi \in H^{2+s}(\Omega)$ and*

$$\|\psi\|_{2+s,\Omega} \leq \widetilde{C}\|f\|_{0,\Omega}.$$

3. The virtual element scheme

In the present section, we will introduce a C^1-virtual element discretization for the numerical approximation of (2.8). The discrete method will be based on the virtual space introduced in [4] for the Cahn–Hilliard equation.

We begin with some notations and assumptions to construct the projectors on polynomial spaces, which are going to be used to build a conforming virtual space of X and to construct the respective discrete bilinear forms, the discrete trilinear form and the discrete functional. Finally, we prove existence and uniqueness of the discrete formulation by using the Banach fixed-point Theorem.

Let $\{\Omega_h\}_h$ be a sequence of decompositions of Ω into general polygonal elements K. We will denote by h_K the diameter of the element K and by h the maximum of the diameters of all the elements of the mesh, i.e.,

$$h := \max_{K\in\Omega_h} h_K.$$

Also, we denote by N_K the number of vertices of K, by e a generic edge of Ω_h and for all $e \in \partial K$, we define a unit normal vector $\boldsymbol{n}_K^e$ that points outside of K and a unit tangent vector $\boldsymbol{t}_K^e$.

3.1. Virtual spaces and polynomial projections

Now, for every polygon $K \in \Omega_h$, we introduce the following preliminary augmented local virtual space (see [4]):

$$\widetilde{X}_h(K) := \left\{ \phi_h \in H^2(K) : \Delta^2\phi_h \in \mathcal{P}_2(K), \phi_h|_{\partial K} \in C^0(\partial K), \phi_h|_e \in \mathcal{P}_3(e)\ \forall e \in \partial K, \nabla\phi_h|_{\partial K} \in [C^0(\partial K)]^2, \partial_{\boldsymbol{n}_K^e}\phi_h|_e \in \mathcal{P}_1(e)\ \forall e \in \partial K \right\}.$$

Next, for a given $\phi_h \in \widetilde{X}_h(K)$, we introduce two sets $\mathbf{O_1}$ and $\mathbf{O_2}$ of linear operators from the local virtual space $\widetilde{X}_h(K)$ into $\mathbb{R}$:

- $\mathbf{O_1}$: contains linear operators evaluating ϕ_h at the N_K vertices of K;
- $\mathbf{O_2}$: contains linear operators evaluating $\nabla\phi_h$ at the N_K vertices of K.

Now, we decompose the bilinear form $A(\cdot,\cdot)$ as follows:

$$A(\varphi,\phi) = \sum_{K\in\Omega_h} A^K(\varphi,\phi) \qquad \forall\varphi,\phi \in X, \tag{3.1}$$

where

$$A^K(\varphi,\phi) = \int_K \mathrm{D}^2\varphi : \mathrm{D}^2\phi \qquad \forall\varphi,\phi \in H^2(K). \tag{3.2}$$

In a similar way, we can decompose the forms $B(\cdot;\cdot,\cdot)$ and $C_{\text{skew}}(\cdot,\cdot)$, with the following local forms:

$$B^K(\zeta;\psi,\phi) := \int_K \Delta\zeta\, \mathbf{curl}\,\psi \cdot \nabla\phi \qquad \forall\zeta,\psi,\phi \in H^2(K), \tag{3.3}$$

$$C^K_{\text{skew}}(\psi,\phi) = \frac{1}{2}\int_K \partial_x\psi\,\phi - \frac{1}{2}\int_K \partial_x\phi\,\psi \qquad \forall\psi,\phi \in H^2(K). \tag{3.4}$$

Projection operators The next step is to build some projector operators from the local virtual space onto $\mathcal{P}_2(K)$ to construct the discrete version of the local bilinear forms and trilinear form along with the discrete load term. The first projector will be constructed by using the local bilinear form (3.2). Indeed, for each polygon K, we define the projector $\Pi_K^{2,\mathrm{D}} : \widetilde{X}_h(K) \to \mathcal{P}_2(K) \subseteq \widetilde{X}_h(K)$ as follows: for each $\phi_h \in \widetilde{X}_h(K)$, $\Pi_K^{2,\mathrm{D}}\phi_h \in \mathcal{P}_2(K)$ is the solution of the following local problem (on each polygon K):

$$A^K(\Pi_K^{2,\mathrm{D}}\phi_h, q) = A^K(\phi_h, q) \quad \forall q \in \mathcal{P}_2(K),$$
$$((\Pi_K^{2,\mathrm{D}}\phi_h, q))_K = ((\phi_h, q))_K \quad \forall q \in \mathcal{P}_1(K),$$

where $((\varphi_h,\phi_h))_K$ is defined as follows:

$$((\varphi_h,\phi_h))_K := \sum_{i=1}^{N_K} \varphi_h(\mathrm{v}_i)\phi_h(\mathrm{v}_i) \qquad \forall\varphi_h,\phi_h \in C^0(\partial K),$$

with v_i, $1 \le i \le N_K$, being the vertices of K.

The following result establishes that the projector $\Pi_K^{2,\mathrm{D}}$ is computable using of the sets $\mathbf{O_1}$ and $\mathbf{O_2}$ (see [4]).

Lemma 3.1. *The operator $\Pi_K^{2,\mathrm{D}} : \widetilde{X}_h(K) \to \mathcal{P}_2(K)$ is explicitly computable for every $\phi_h \in \widetilde{X}_h(K)$, using only the information of the linear operators $\mathbf{O_1}$ and $\mathbf{O_2}$.*

Next, we introduce, for each $K \in \Omega_h$, our local enhanced virtual space as follows:

$$X_h(K) := \left\{ \phi_h \in \widetilde{X}_h(K) : (\phi_h - \Pi_K^{2,\mathrm{D}}\phi_h, q)_{0,K} = 0, \quad \forall q \in \mathcal{P}_2(K) \right\}.$$

In the space $X_h(K)$, we have the following properties (for further details, see [4]):

- the sets of linear operators $\mathbf{O_1}$ and $\mathbf{O_2}$ constitutes a set of degrees of freedom;
- $\Pi_K^{2,\mathrm{D}}$ is well defined and it is computable using the information of the degrees of freedom $\mathbf{O_1}$ and $\mathbf{O_2}$.

Now, for each $K\in\Omega_h$, we consider the L^2-projection onto $\mathcal{P}_2(K)$, defined as follows: for each $\phi\in L^2(K), \Pi_2^K\phi\in\mathcal{P}_2(K)$ is the unique function such that

$$\int_K q\Pi_2^K\phi=\int_K q\phi \qquad \forall q\in\mathcal{P}_2(K). \tag{3.5}$$

We observe that, using the definition of the local space $X_h(K)$, for each $\phi\in X_h(K)$, the polynomial function $\Pi_2^K\phi\in\mathcal{P}_2(K)$ is fully computable. In fact, due to the particular property appearing in the definition of space $X_h(K)$, the right hand side in (3.5) is computable using $\Pi_K^{2,\mathrm{D}}\phi$. Actually, it is easy to check that on the space $X_h(K)$ the projectors $\Pi_2^K\phi$ and $\Pi_K^{2,\mathrm{D}}\phi$ are the same operator. In fact:

$$\int_K q\Pi_2^K\phi=\int_K q\,\Pi_K^{2,\mathrm{D}}\phi \qquad \forall q\in\mathcal{P}_2(K). \tag{3.6}$$

Now, we will consider the following projection onto the polynomial space $[\mathcal{P}_1(K)]^2$: we define $\boldsymbol{\Pi}_1^K:[L^2(K)]^2\to[\mathcal{P}_1(K)]^2$, for each $\boldsymbol{v}\in[L^2(K)]^2$ by

$$\int_K \boldsymbol{\Pi}_1^K\boldsymbol{v}\cdot\boldsymbol{q}=\int_K \boldsymbol{v}\cdot\boldsymbol{q} \qquad \forall \boldsymbol{q}\in[\mathcal{P}_1(K)]^2. \tag{3.7}$$

Using integration by parts, it is easy to see that for any $\phi_h\in X_h(K)$, the vector functions $\boldsymbol{\Pi}_1^K\mathbf{curl}\,\phi_h\in[\mathcal{P}_1(K)]^2$ and $\boldsymbol{\Pi}_1^K\nabla\phi_h\in[\mathcal{P}_1(K)]^2$ can be explicitly computed from the degrees of freedom $\mathbf{O_1}$ and $\mathbf{O_2}$. In fact, for all $K\in\Omega_h$ and for all $\phi_h\in X_h(K)$, using integration by parts on the right hand side of (3.7) (with $\mathbf{curl}\,\phi_h$ instead of $\boldsymbol{v}$), we have

$$\begin{aligned}\int_K \mathbf{curl}\,\phi_h\cdot\boldsymbol{q}&=\int_K\phi_h\,\mathrm{rot}\,\boldsymbol{q}-\int_{\partial K}\phi_h(\boldsymbol{q}\cdot\boldsymbol{t}_K^e) \qquad \forall\boldsymbol{q}\in[\mathcal{P}_1(K)]^2\\ &=\mathrm{rot}\,\boldsymbol{q}\int_K(\Pi_K^{2,\mathrm{D}}\phi_h)-\int_{\partial K}\phi_h(\boldsymbol{q}\cdot\boldsymbol{t}_K^e) \qquad \forall\boldsymbol{q}\in[\mathcal{P}_1(K)]^2,\end{aligned}$$

where we have used the definition of $\Pi_2^K\phi_h$ and (3.6). The first term on the right hand side above depends only on $\Pi_K^{2,\mathrm{D}}\phi_h$ and this depends only on the values of the degrees of freedom (see Lemma 3.1). The second term is an integral on the boundary of the element K, which is fully computable. Similarly, we have that $\boldsymbol{\Pi}_1^K\nabla\phi_h$ is fully computable from the degrees of freedom.

Also, we note that for each $\phi_h\in X_h(K)$ the projection function $\Pi_0^K\Delta\phi_h\in\mathcal{P}_0(K)$ is computable using the degrees of freedom $\mathbf{O_1}$ and $\mathbf{O_2}$. Indeed, for each $\phi_h\in X_h(K)$ and for all $q_0\in\mathcal{P}_0(K)$ we have

$$\int_K q_0\,\Pi_0^K\Delta\phi_h=\int_K q_0\,\Delta\phi_h=\int_{\partial K}q_0\,\partial_n\phi_h,$$

from the equality above we have that

$$\Pi_0^K\Delta\phi_h=\frac{1}{|K|}\int_{\partial K}\partial_n\phi_h,$$

where $|K|$ denotes the area of polygon K.

Now, by combining the local spaces $X_h(K)$ and incorporating the homogeneous Dirichlet boundary conditions, we define the global virtual space for the numerical approximation of (2.8): for every decomposition Ω_h of Ω into polygons K, we define

$$X_h:=\left\{\phi_h\in X:\ \phi_h|_K\in X_h(K)\right\}.$$

The degrees of freedom for X_h are:

- $\mathbf{OG_1}$: pointwise values of ϕ_h on all vertices of Ω_h excluding the vertices on Γ;
- $\mathbf{OG_2}$: pointwise values of $\nabla\phi_h$ on all vertices of Ω_h excluding the vertices on Γ.

3.2. Construction of the discrete forms

In this section, we will construct the discrete version of the continuous bilinear forms, the trilinear form and the right-hand side, using the projection operators introduced in Section 3.1.

First, let $S_{\mathrm{D}}^K(\cdot,\cdot)$ be any symmetric positive definite bilinear form to be chosen as to satisfy:

$$c_0A^K(\phi_h,\phi_h)\le S_{\mathrm{D}}^K(\phi_h,\phi_h)\le c_1A^K(\phi_h,\phi_h) \qquad \forall\phi_h\in X_h(K),\ \text{with}\ \ \Pi_K^{2,\mathrm{D}}\phi_h=0, \tag{3.8}$$

with c_0 and c_1 positive constants independent of h and K.

Now, using the projector operator $\Pi_K^{2,\mathrm{D}}$ and the bilinear form $S_{\mathrm{D}}^K(\cdot,\cdot)$, we introduce the following computable discrete local bilinear form:

$$A^{h,K}(\psi_h,\phi_h):=A^K\left(\Pi_K^{2,\mathrm{D}}\psi_h,\Pi_K^{2,\mathrm{D}}\phi_h\right)+S_{\mathrm{D}}^K\left(\psi_h-\Pi_K^{2,\mathrm{D}}\psi_h,\phi_h-\Pi_K^{2,\mathrm{D}}\phi_h\right), \tag{3.9}$$

as an approximation of the continuous bilinear form $A^K(\cdot,\cdot)$ (cf. (3.1)).

We choose the following representation for the bilinear form $S_{\rm D}^K(\cdot,\cdot)$ satisfying (3.8) (see [4,44]):

$$S_{\rm D}^K(\psi_h,\phi_h) := \sigma_{\rm D}^K \sum_{i=1}^{N_K} \left[\psi_h(\mathbf{v}_i)\phi_h(\mathbf{v}_i) + h_{\mathbf{v}_i}^2 \nabla\psi_h(\mathbf{v}_i)\cdot\nabla\phi_h(\mathbf{v}_i)\right] \quad \forall \psi_h,\phi_h \in X_h(K),$$

where $\mathbf{v}_1,\dots,\mathbf{v}_{N_K}$ are the vertices of the element K, $h_{\mathbf{v}_i}$ corresponds to the maximum diameter of the elements with $\mathbf{v}_i$ as a vertex. The parameter $\sigma_{\rm D}^K$ is a multiplicative factor to take into account the h-scaling, for instance, in the numerical test we have taken $\sigma_{\rm D}^K$ as the trace of the matrix $A^K(\Pi_K^{2,{\rm D}}\psi_h,\Pi_K^{2,{\rm D}}\phi_h)$ (cf. (3.9)).

For the approximation of the local trilinear form $B^K(\cdot;\cdot,\cdot)$ (cf. (3.3)), we consider the following computable form:

$$B^{h,K}(\zeta_h;\psi_h,\phi_h) := \int_K \left[\left(\Pi_0^K\Delta\zeta_h\right)\left(\boldsymbol{\Pi}_1^K\mathbf{curl}\,\psi_h\right)\right]\cdot\boldsymbol{\Pi}_1^K\nabla\phi_h \qquad \forall\zeta_h,\psi_h,\phi_h\in X_h(K). \tag{3.10}$$

For the approximation of the bilinear form $C_{\rm skew}^K(\cdot,\cdot)$ (cf. (3.4)), we consider the skew-symmetric discrete local form:

$$C_{\rm skew}^{h,K}(\psi_h,\phi_h) := \frac{1}{2}\int_K \Pi_2^K(\partial_x\psi_h)\,\Pi_2^K\phi_h - \frac{1}{2}\int_K \Pi_2^K\psi_h\,\Pi_2^K(\partial_x\phi_h). \tag{3.11}$$

We recall that all the above forms are computable using only the degrees of freedom $\mathbf{O_1}$ and $\mathbf{O_2}$.

Then, we define the global bilinear forms and trilinear form as follows:

$$A^h : X_h\times X_h\to\mathbb{R},\quad A^h(\psi_h,\phi_h) := \sum_{K\in\Omega_h} A^{h,K}(\psi_h,\phi_h), \tag{3.12}$$

$$B^h : X_h\times X_h\times X_h\to\mathbb{R},\quad B^h(\zeta_h;\psi_h,\phi_h) := \sum_{K\in\Omega_h} B^{h,K}(\zeta_h;\psi_h,\phi_h), \tag{3.13}$$

$$C_{\rm skew}^h : X_h\times X_h\to\mathbb{R},\quad C_{\rm skew}^h(\psi_h,\phi_h) := \sum_{K\in\Omega_h} C_{\rm skew}^{h,K}(\psi_h,\phi_h), \tag{3.14}$$

for all $\zeta_h,\psi_h,\phi_h\in X_h$. Moreover, we observe that the forms $B^h(\cdot;\cdot,\cdot)$ and $C_{\rm skew}^h(\cdot,\cdot)$ can be extended to the whole X.

The next step consists in constructing a computable approximation of the right hand side (2.6), using the sets of degrees of freedom $\mathbf{O_1}$ and $\mathbf{O_2}$. With this aim, for each element K we define the following term:

$$F^{h,K}(\phi_h) := \int_K \Pi_2^K f\,\phi_h \equiv \int_K f\,\Pi_2^K\phi_h \qquad \forall\phi_h\in X_h(K),$$

where we have used the L^2-projection operator (3.5). Thus, we introduce the following approximation for the functional defined in (2.6):

$$F^h(\phi_h) := \sum_{K\in\Omega_h} F^{h,K}(\phi_h) \qquad \forall\phi_h\in X_h. \tag{3.15}$$

The following result establishes the classical consistency and stability properties for the discrete local bilinear forms.

Proposition 3.1. *The local bilinear forms $A^K(\cdot,\cdot)$, $A^{h,K}(\cdot,\cdot)$, $C_{\rm skew}^K(\cdot,\cdot)$ and $C_{\rm skew}^{h,K}(\cdot,\cdot)$, defined in (3.2), (3.9), (3.4) and (3.11), respectively, on each element K satisfies the following properties:*

- *Consistency: for all $h>0$ and for all $K\in\Omega_h$, we have that*

$$A^{h,K}(q,\phi_h) = A^K(q,\phi_h) \qquad \forall q\in\mathcal{P}_2(K), \qquad \forall\phi_h\in X_h(K), \tag{3.16}$$

$$C_{\rm skew}^{h,K}(q,\phi_h) = C_{\rm skew}^K(q,\phi_h) \qquad \forall q\in\mathcal{P}_2(K), \qquad \forall\phi_h\in X_h(K), \tag{3.17}$$

- *Stability and boundedness: There exist positive constants α_1 and α_2, independent of h and K, such that:*

$$\alpha_1 A^K(\phi_h,\phi_h) \le A^{h,K}(\phi_h,\phi_h) \le \alpha_2 A^K(\phi_h,\phi_h) \qquad \forall\phi_h\in X_h(K). \tag{3.18}$$

Proof. The proof follows basically from the definition of the bilinear forms. We omit further details and refer to [4,5]. □

The following lemma, which can be seen as the discrete version of Lemma 2.1, establishes additional properties for the discrete forms.

Lemma 3.2. *There exist positive constants $\widehat{C_{B^h}}$, $\widehat{C}_2$ and C_1, independent of h, such that the forms defined in (3.12)-(3.15) satisfy the following properties:*

$$|A^h(\psi_h,\phi_h)| \le \alpha_2\,\|\psi_h\|_X\|\phi_h\|_X \qquad \forall\psi_h,\phi_h\in X_h, \tag{3.19}$$

$$A^h(\phi_h,\phi_h) \ge \alpha_1\,\|\phi_h\|_X^2 \qquad \forall\phi_h\in X_h, \tag{3.20}$$

$$B^h(\zeta_h;\psi_h,\phi_h) \le \widehat{C_{B^h}}\,\|\zeta_h\|_X\|\psi_h\|_X\|\phi_h\|_X \qquad \forall\zeta_h,\psi_h,\phi_h\in X_h, \tag{3.21}$$

$$B^h(\zeta_h;\phi_h,\phi_h) = 0 \qquad \forall\zeta_h,\phi_h\in X_h, \tag{3.22}$$

$$|C_{\rm skew}^h(\psi_h,\phi_h)| \le \widehat{C}_2\,\|\psi_h\|_X\|\phi_h\|_X \qquad \forall\psi_h,\phi_h\in X_h, \tag{3.23}$$

$$C_{\rm skew}^h(\phi_h,\phi_h) = 0 \qquad \forall\phi_h\in X_h, \tag{3.24}$$

$$|F^h(\phi_h)| \le C_1\|f\|_{0,\Omega}\|\phi_h\|_X \qquad \forall\psi_h,\phi_h\in X_h. \tag{3.25}$$

Proof. Properties (3.19) and (3.20) follow from (3.18) and the ellipticity of the bilinear form $A^K(\cdot,\cdot)$. To prove property (3.21), we use the definition of the trilinear form $B^h(\cdot;\cdot,\cdot)$ (cf. (3.13)) and Hölder inequality, we have

$$\begin{aligned} B^h(\zeta_h;\psi_h,\phi_h) &= \sum_{K\in\Omega_h}\int_K \left[\left(\Pi_0^K\Delta\zeta_h\right)\left(\boldsymbol{\Pi}_1^K\,\mathbf{curl}\,\psi_h\right)\right]\cdot\boldsymbol{\Pi}_1^K\nabla\phi_h \\ &\le \sum_{K\in\Omega_h}\|\Pi_0^K\Delta\zeta_h\|_{0,K}\|\boldsymbol{\Pi}_1^K\,\mathbf{curl}\,\psi_h\|_{L^4(K)}\|\boldsymbol{\Pi}_1^K\nabla\phi_h\|_{L^4(K)}. \end{aligned}$$

Using the continuity of the operator Π_0^K with respect to the L^2-norm and the continuity of the operator $\boldsymbol{\Pi}_1^K$ with respect to the norm L^4-norm (see [8]), we have

$$B^h(\zeta_h;\psi_h,\phi_h)\le C\sum_{K\in\Omega_h}\|\Delta\zeta_h\|_{0,K}\|\mathbf{curl}\,\psi_h\|_{L^4(K)}\|\nabla\phi_h\|_{L^4(K)}.$$

Now, applying the Hölder inequality (for sequences), we obtain

$$\begin{aligned} B^h(\zeta_h;\psi_h,\phi_h) &\le C\left(\sum_{K\in\Omega_h}\|\Delta\zeta_h\|_{0,K}^2\right)^{1/2}\left(\sum_{K\in\Omega_h}\|\mathbf{curl}\,\psi_h\|_{L^4(K)}^4\right)^{1/4}\left(\sum_{K\in\Omega_h}\|\nabla\phi_h\|_{L^4(K)}^4\right)^{1/4} \\ &\le C\|\Delta\zeta_h\|_{0,\Omega}\|\mathbf{curl}\,\psi_h\|_{L^4(\Omega)}\|\nabla\phi_h\|_{L^4(\Omega)}. \end{aligned}$$

Then, by Sobolev embedding theorem, it holds that

$$B^h(\zeta_h;\psi_h,\phi_h)\le\widehat{C_{B^h}}\|\zeta_h\|_X\|\psi_h\|_X\|\phi_h\|_X,$$

where $\widehat{C_{B^h}}$ is a constant independent of h.

Finally, (3.22)-(3.25) follow from the definition of the corresponding forms. We conclude the proof. □

3.3. Discrete problem and fixed-point strategy

In this section, we will write the discrete VEM formulation to solve the quasi-geostrophic equations presented in (2.8). Our scheme will be based on the discrete forms and the results introduced in the previous section. Then, we will analyze a point-fixed strategy to establish the existence and uniqueness of the discrete virtual scheme.

The discrete problem reads as follows: find $\psi_h\in X_h$, such that

$$\mathrm{Re}^{-1}A^h(\psi_h,\phi_h)+B^h(\psi_h;\psi_h,\phi_h)-\mathrm{Ro}^{-1}C_{\mathrm{skew}}^h(\psi_h,\phi_h)=\mathrm{Ro}^{-1}F^h(\phi_h)\qquad\forall\phi_h\in X_h,\tag{3.26}$$

where $A^h(\cdot,\cdot)$ and $C_{\mathrm{skew}}^h(\cdot,\cdot)$ are the discrete bilinear forms defined in (3.12) and (3.14), respectively, $B^h(\cdot;\cdot,\cdot)$ is the discrete trilinear form defined in (3.13), and $F^h(\cdot)$ is the functional introduced in (3.15).

In order to prove well posedness of (3.26), we are going to use, as in the continuous case, a fixed-point strategy. Indeed, given $\zeta_h\in X_h$, we define the following operator

$$\begin{aligned} T^h: X_h &\longrightarrow X_h \\ \zeta_h &\longmapsto T^h(\zeta_h)=\varphi_h, \end{aligned}$$

where φ_h is the solution of the following linear problem: find $\varphi_h\in X_h$ such that

$$\mathcal{Q}_{\zeta_h}(\varphi_h,\phi_h)=\mathrm{Ro}^{-1}F^h(\phi_h)\qquad\forall\phi_h\in X_h,\tag{3.27}$$

where the bilinear form $\mathcal{Q}_{\zeta_h}(\cdot,\cdot)$ is given by

$$\mathcal{Q}_{\zeta_h}(\varphi_h,\phi_h):=\mathrm{Re}^{-1}A^h(\varphi_h,\phi_h)+B^h(\zeta_h;\varphi_h,\phi_h)-\mathrm{Ro}^{-1}C_{\mathrm{skew}}^h(\varphi_h,\phi_h).$$

The following lemma establishes that the operator T^h is well-defined.

Lemma 3.3. *Given $\zeta_h\in X_h$, there exists a unique $\varphi_h\in X_h$ such that $T^h(\zeta_h)=\varphi_h$.*

Proof. We are going to use the Lax-Milgram Theorem to prove that problem (3.27) is well-posed. Indeed, using the properties (3.19), (3.21) and (3.23), we have that $\mathcal{Q}_{\zeta_h}(\cdot,\cdot)$ is bounded with a positive constant independent of h. On the other hand, for each $\phi_h\in X_h$, using (3.22) and (3.24), we have

$$\begin{aligned} \mathcal{Q}_{\zeta_h}(\phi_h,\phi_h) &= \mathrm{Re}^{-1}A^h(\phi_h,\phi_h)+B^h(\zeta_h;\phi_h,\phi_h)-\mathrm{Ro}^{-1}C_{\mathrm{skew}}^h(\phi_h,\phi_h) \\ &= \mathrm{Re}^{-1}A^h(\phi_h,\phi_h) \\ &\ge \mathrm{Re}^{-1}\alpha_1\|\phi_h\|_X^2, \end{aligned}$$

where (3.20) has been used in the last inequality. Thus, by a direct application of the Lax-Milgram Theorem, we conclude that problem (3.27) has a unique solution $\varphi_h\in X_h$. Moreover, from the definition of the discrete problem (cf. (3.27)), (3.22), (3.24) and (3.25), the following estimate holds

$$\|\varphi_h\|_X\le C_1\alpha_1^{-1}\,\mathrm{Ro}^{-1}\mathrm{Re}\,\|f\|_{0,\Omega}.$$

Therefore, operator T^h is well-defined. □

Now, we introduce the following set

$$\mathcal{N}_h := \{\phi_h \in X_h : \|\phi_h\|_X \leq R\},$$

where $R := C_1\alpha_1^{-1}\,\mathrm{Ro}^{-1}\mathrm{Re}\,\|f\|_{0,\Omega}$. As an immediate consequence of the previous lemma, we have that $T^h(\mathcal{N}_h) \subseteq \mathcal{N}_h$.

Note that our discrete virtual scheme (3.26) is well-posed if only if operator T^h has a unique fixed point in $\mathcal{N}_h$.

The following lemma establishes that T^h is a contraction mapping in $\mathcal{N}_h$.

Lemma 3.4. *Assume that*

$$\frac{\widehat{C_{B^h}}C_1\mathrm{Ro}^{-1}\mathrm{Re}^2\|f\|_{0,\Omega}}{\alpha_1^2} < 1. \tag{3.28}$$

Then, T^h is a contraction mapping in $\mathcal{N}_h$.

Proof. Let $\zeta_h^1, \psi_h^1, \zeta_h^2, \psi_h^2 \in \mathcal{N}_h$, such that $T^h(\zeta_h^1) = \psi_h^1$ and $T^h(\zeta_h^2) = \psi_h^2$, then from the definition of the operator $T^h(\cdot)$, we have

$$\mathrm{Re}^{-1}A^h(\psi_h^1,\phi_h) + B^h(\zeta_h^1;\psi_h^1,\phi_h) - \mathrm{Ro}^{-1}C^h_{\mathrm{skew}}(\psi_h^1,\phi_h) = \mathrm{Ro}^{-1}F^h(\phi_h) \qquad \forall \phi_h \in \mathcal{N}_h, \tag{3.29}$$

$$\mathrm{Re}^{-1}A^h(\psi_h^2,\phi_h) + B^h(\zeta_h^2;\psi_h^2,\phi_h) - \mathrm{Ro}^{-1}C^h_{\mathrm{skew}}(\psi_h^2,\phi_h) = \mathrm{Ro}^{-1}F^h(\phi_h) \qquad \forall \phi_h \in \mathcal{N}_h. \tag{3.30}$$

Subtracting (3.30) from (3.29), due to the properties of the bilinear forms $A^h(\cdot,\cdot)$ and $C^h_{\mathrm{skew}}(\cdot,\cdot)$, we have that

$$\mathrm{Re}^{-1}A^h(\psi_h^1-\psi_h^2,\phi_h) + [B^h(\zeta_h^1;\psi_h^1,\phi_h) - B^h(\zeta_h^2;\psi_h^2,\phi_h)] - \mathrm{Ro}^{-1}C^h_{\mathrm{skew}}(\psi_h^1-\psi_h^2,\phi_h) = 0,$$

for all $\phi_h \in \mathcal{N}_h$. Now, taking $\phi_h := \psi_h^1 - \psi_h^2$ in the above equality, we have that $C^h_{\mathrm{skew}}(\cdot,\cdot)$ vanishes (cf. (3.24)). Thus, we obtain

$$\mathrm{Re}^{-1}A^h(\psi_h^1-\psi_h^2,\psi_h^1-\psi_h^2) + B^h(\zeta_h^1;\psi_h^1,\psi_h^1-\psi_h^2) - B^h(\zeta_h^2;\psi_h^2,\psi_h^1-\psi_h^2) = 0.$$

Then, adding and subtracting ψ_h^2 in the second term of the left hand above, we get

$$\begin{aligned}
0 &= \mathrm{Re}^{-1}A^h(\psi_h^1-\psi_h^2,\psi_h^1-\psi_h^2) + B^h(\zeta_h^1;\psi_h^1-\psi_h^2,\psi_h^1-\psi_h^2) + B^h(\zeta_h^1;\psi_h^2,\psi_h^1-\psi_h^2) - B^h(\zeta_h^2;\psi_h^2,\psi_h^1-\psi_h^2)\\
&= \mathrm{Re}^{-1}A^h(\psi_h^1-\psi_h^2,\psi_h^1-\psi_h^2) + B^h(\zeta_h^1;\psi_h^2,\psi_h^1-\psi_h^2) - B^h(\zeta_h^2;\psi_h^2,\psi_h^1-\psi_h^2)\\
&= \mathrm{Re}^{-1}A^h(\psi_h^1-\psi_h^2,\psi_h^1-\psi_h^2) + B^h(\zeta_h^1-\zeta_h^2;\psi_h^2,\psi_h^1-\psi_h^2),
\end{aligned}$$

where we have used (3.22). Then, we have

$$\mathrm{Re}^{-1}A^h(\psi_h^1-\psi_h^2,\psi_h^1-\psi_h^2) = -B^h(\zeta_h^1-\zeta_h^2;\psi_h^2,\psi_h^1-\psi_h^2),$$

then applying the Cauchy-Schwarz inequality, (3.20) and (3.21), we obtain

$$\mathrm{Re}^{-1}\alpha_1\|\psi_h^1-\psi_h^2\|_X^2 \leq \widehat{C_{B^h}}\|\psi_h^2\|_X\|\zeta_h^1-\zeta_h^2\|_X\|\psi_h^1-\psi_h^2\|_X,$$

using the fact that $\psi_h^2 \in \mathcal{N}_h$, we obtain

$$\|\psi_h^1-\psi_h^2\|_X \leq \frac{\widehat{C_{B^h}}C_1\mathrm{Ro}^{-1}\mathrm{Re}^2\|f\|_{0,\Omega}}{\alpha_1^2}\|\zeta_h^1-\zeta_h^2\|_X.$$

Thus, according to assumption (3.28), we have that T^h is a contraction mapping. The proof is complete. □

The following result is a direct consequence of Lemma 3.4 and the Banach fixed-point Theorem.

Theorem 3.1. *If*

$$\lambda_h := \frac{\widehat{C_{B^h}}C_1\mathrm{Ro}^{-1}\mathrm{Re}^2\|f\|_{0,\Omega}}{\alpha_1^2} < 1, \tag{3.31}$$

there exists a unique $\psi_h \in \mathcal{N}_h$ solution to problem (3.26), which satisfies the following continuous dependence

$$\|\psi_h\|_X \leq \frac{C_1\mathrm{Ro}^{-1}\mathrm{Re}\,\|f\|_{0,\Omega}}{\alpha_1}.$$

4. Convergence analysis

In this section, we will analyze the convergence properties of the discrete virtual element scheme presented in Section 3.3. In the forthcoming analysis, we will make the following assumptions for the polygonal mesh Ω_h: there exists a real number $C_{\Omega_h} > 0$ such that, for every h and every $K \in \Omega_h$ we have

A1: $K \in \Omega_h$ is star-shaped with respect to every point of a ball of radius $C_{\Omega_h}h_K$;
A2: the ratio between the shortest edge and the diameter h_K of K is larger than C_{Ω_h}.

We introduce the following broken H^{ℓ}-seminorm, for each integer $\ell \geq 0$:

$$|\phi|_{\ell,h} := \left(\sum_{K\in\Omega_h} |\phi|^2_{\ell,K} \right)^{1/2},$$

which is well defined for every $\phi \in L^2(\Omega)$ such that $\phi|_K \in H^{\ell}(K)$ for all polygon $K \in \Omega_h$.

The following approximation results will play a relevant role in our error analysis (see [4,9,12]).

Proposition 4.1. *Assume* **A2** *is satisfied, then there exists a constant $C > 0$, such that for every $\phi \in H^{\delta}(K)$, there exists $\phi_{\pi} \in \mathcal{P}_2(K)$, such that*

$$|\phi - \phi_{\pi}|_{\ell,K} \leq C h_K^{\delta-\ell} |\phi|_{\delta,K}, \quad 0 \leq \delta \leq 3,\ \ell = 0, 1, \dots, [\delta],$$

where $[\delta]$ denotes the largest integer equal to or smaller than $\delta \in \mathbb{R}$.

Proposition 4.2. *Assume that* **A1** – **A2** *are satisfied. Then, for each $\phi \in H^{2+s}(\Omega)$, with $s \in (1/2, 1]$ there exist $\phi_I \in X_h$ and $C > 0$, independent of h, such that*

$$\|\phi - \phi_I\|_X \leq C h^s |\phi|_{2+s,\Omega}.$$

Proof. The proof follows repeating the arguments from [9, Proposition 4.2] (see also [4, Proposition 3.1]). □

We will also use the following approximation property (see [8]):

Lemma 4.1. *Let $K \in \Omega_h$, and δ, p two real numbers such that $0 \leq \delta \leq 1$ and $0 \leq p \leq \infty$. Then, there exists a constant $C > 0$, independent of h_K, such that for every $\boldsymbol{v} \in [H^{\delta}(K)]^2$*

$$|\boldsymbol{v} - \boldsymbol{\Pi}_1^K \boldsymbol{v}|_{L^p(K)} \leq C h_K^{\delta} |\boldsymbol{v}|_{W^{\delta,p}(K)}.$$

Now, we start with the following bound.

Proposition 4.3. *Let $f \in L^2(\Omega)$ and let $F(\cdot)$ and $F^h(\cdot)$ be the functionals defined in (2.6) and (3.15), respectively. Then, we have the following estimate:*

$$\left\| F - F^h \right\|_{X_h'} := \sup_{\substack{\phi_h \in X_h \\ \phi_h \neq 0}} \frac{|F(\phi_h) - F^h(\phi_h)|}{\|\phi_h\|_X} \leq C h^2 \|f\|_{0,\Omega}.$$

Proof. The proof follows from the definition of the functionals $F(\cdot)$ and $F^h(\cdot)$, together with approximation properties of the projector Π_2^K. □

The next step is to establish two technical results for the trilinear forms $B(\cdot;\cdot,\cdot)$ and $B^h(\cdot;\cdot,\cdot)$. We begin with the following lemma.

Lemma 4.2. *Let $v \in H^{2+s}(\Omega) \cap X$, with $s \in (1/2, 1]$. Then for all $w \in X$, we have that*

$$|B(v; v, w) - B^h(v; v, w)| \leq C h^s (\|v\|_{1+s,\Omega} + \|v\|_X) \|v\|_{2+s,\Omega} \|w\|_X.$$

Proof. Let $v \in H^{2+s}(\Omega) \cap X$ and $w \in X$, then adding and subtracting suitable terms and using orthogonality properties of the projectors Π_0^K and $\boldsymbol{\Pi}_1^K$, we have that

$$\begin{aligned} B(v; v, w) - B^h(v; v, w) &= \sum_{K\in\Omega_h} \int_K \left[\Delta v \,\mathbf{curl}\, v \cdot \nabla w - \left(\Pi_0^K \Delta v \,\boldsymbol{\Pi}_1^K \mathbf{curl}\, v \right) \cdot \boldsymbol{\Pi}_1^K \nabla w \right] \\ &= \sum_{K\in\Omega_h} \int_K \Delta v \,\mathbf{curl}\, v \cdot \left(\nabla w - \boldsymbol{\Pi}_1^K \nabla w \right) + \sum_{K\in\Omega_h} \int_K \left(\Delta v \left(\mathbf{curl}\, v - \boldsymbol{\Pi}_1^K \mathbf{curl}\, v \right) \right) \cdot \boldsymbol{\Pi}_1^K \nabla w \\ &\quad + \sum_{K\in\Omega_h} \int_K \left(\left(\Delta v - \Pi_0^K \Delta v \right) \boldsymbol{\Pi}_1^K \mathbf{curl}\, v \right) \cdot \boldsymbol{\Pi}_1^K \nabla w \\ &=: T_1 + T_2 + T_3. \end{aligned} \tag{4.1}$$

We will bound the terms in the last equality. Applying Hölder inequality and approximation properties of projector $\boldsymbol{\Pi}_1^K$ (see Lemma 4.1), we bound the term T_1 as follows

$$\begin{aligned} T_1 &\leq \sum_{K\in\Omega_h} C \|\Delta v\|_{L^4(K)} \|\mathbf{curl}\, v\|_{L^4(K)} \|\nabla w - \boldsymbol{\Pi}_1^K \nabla w\|_{0,K} \\ &\leq \sum_{K\in\Omega_h} C \|\Delta v\|_{L^4(K)} \|\mathbf{curl}\, v\|_{L^4(K)} C h |\nabla w|_{1,K}, \end{aligned}$$

then using Hölder inequality (for sequences) and the fact that $H^s(\Omega) \hookrightarrow L^4(\Omega)$, we obtain that

$$T_1 \le Ch\left(\sum_{K\in\Omega_h}\|\Delta v\|^4_{L^4(K)}\right)^{1/4}\left(\sum_{K\in\Omega_h}\|\mathbf{curl}\, v\|^4_{L^4(K)}\right)^{1/4}\left(\sum_{K\in\Omega_h}|w|^2_{2,K}\right)^{1/2}$$
$$\le Ch\|\Delta v\|_{L^4(\Omega)}\|\mathbf{curl}\, v\|_{L^4(\Omega)}\|w\|_X \tag{4.2}$$
$$\le Ch\|\Delta v\|_{s,\Omega}\|\mathbf{curl}\, v\|_{s,\Omega}\|w\|_X$$
$$\le Ch\|v\|_{2+s,\Omega}\|v\|_{1+s,\Omega}\|w\|_X.$$

Now, for the term T_2, we use again Hölder inequality, approximation properties of projector $\mathbf{\Pi}_1^K$ in Sobolev spaces (see Lemma 4.1), and continuity of $\mathbf{\Pi}_1^K$ with respect L^4-norm (see [8]), to get

$$T_2 \le \sum_{K\in\Omega_h} C\|\Delta v\|_{0,K}\|\mathbf{curl}\, v-\mathbf{\Pi}_1^K\mathbf{curl}\, v\|_{L^4(K)}\|\mathbf{\Pi}_1^K\nabla w\|_{L^4(K)}$$
$$\le \sum_{K\in\Omega_h} C\|\Delta v\|_{0,K}h^s\|\mathbf{curl}\, v\|_{W^{s,4}(K)}\|\nabla w\|_{L^4(K)}.$$

Now, using again Hölder inequality (for sequences) and Sobolev embeddings $H^s(\Omega)\hookrightarrow L^4(\Omega)$ and $H^{1+s}(\Omega)\hookrightarrow W^{s,4}(\Omega)$, we obtain that

$$T_2 \le Ch^s\left(\sum_{K\in\Omega_h}\|\Delta v\|^2_{0,K}\right)^{1/2}\left(\sum_{K\in\Omega_h}\|\mathbf{curl}\, v\|^4_{W^{s,4}(K)}\right)^{1/4}\left(\sum_{K\in\Omega_h}\|\nabla w\|^4_{L^4(K)}\right)^{1/4}$$
$$\le Ch^s\|\Delta v\|_{0,\Omega}|\mathbf{curl}\, v|_{W^{s,4}(\Omega)}\|\nabla w\|_{L^4(\Omega)} \tag{4.3}$$
$$\le Ch^s\|v\|_X|\mathbf{curl}\, v|_{1+s,\Omega}\|w\|_X$$
$$\le Ch^s\|v\|_X\|v\|_{2+s,\Omega}\|w\|_X.$$

We continue with the term T_3. We use Hölder inequality and the continuity of the projector $\mathbf{\Pi}_1^K$ with respect L^4-norm and the approximation property for projector Π_0^K, it holds that

$$T_3 \le \sum_{K\in\Omega_h} C\|\Delta v-\Pi_0^K\Delta v\|_{0,K}\|\mathbf{\Pi}_1^K\mathbf{curl}\, v\|_{L^4(K)}\|\mathbf{\Pi}_1^K\nabla w\|_{L^4(K)}$$
$$\le \sum_{K\in\Omega_h} Ch^s\|\Delta v\|_{s,K}\|\mathbf{curl}\, v\|_{L^4(K)}\|\nabla w\|_{L^4(K)}.$$

By employing the Hölder inequality (for sequences) and Sobolev embedding theorem, we have that

$$T_3 \le Ch^s\|v\|_{2+s,\Omega}|v|_{1+s,\Omega}\|w\|_X. \tag{4.4}$$

Finally, the proof follows from the estimates (4.2), (4.3), (4.4) and (4.1). □

Now, we state the second technical result.

Lemma 4.3. *For all $\zeta,\varphi,\phi\in X$ we have that*

$$|B^h(\varphi;\varphi,\phi)-B^h(\zeta;\zeta,\phi)| \le \widehat{C_{B^h}}\left(\|\zeta\|_X\|\phi\|_X+\|\varphi-\zeta+\phi\|_X(\|\varphi\|_X+\|\zeta\|_X)\right)\|\phi\|_X.$$

Proof. Let $\zeta,\varphi,\phi\in X$. Then, adding and subtracting suitable terms, using the trilinearity of the form $B^h(\cdot;\cdot,\cdot)$ and the property (3.22), we have

$$\begin{aligned}
&B^h(\varphi;\varphi,\phi)-B^h(\zeta;\zeta,\phi)\\
&\quad= B^h(\varphi;\varphi-\zeta,\phi)+B^h(\varphi-\zeta;\zeta,\phi)\\
&\quad= B^h(\varphi;\varphi-\zeta+\phi,\phi)-B^h(\varphi;\phi,\phi)+B^h(\varphi-\zeta+\phi;\zeta,\phi)-B^h(\phi;\zeta,\phi)\\
&\quad= B^h(\varphi;\varphi-\zeta+\phi,\phi)+B^h(\varphi-\zeta+\phi;\zeta,\phi)-B^h(\phi;\zeta,\phi).
\end{aligned}$$

Thus, the proof follows from (3.21) with continuous arguments. □

The following theorem provides the rate of convergence of our virtual element scheme.

Theorem 4.1. *Let ψ and ψ_h be the unique solutions of problem (2.8) and problem (3.26), respectively. Then, there exists a positive constant C, independent of h, such that*

$$\|\psi-\psi_h\|_X \le C\, h^s\mathcal{G}(f;\mathrm{Re},\mathrm{Ro},\lambda,\lambda_h),$$

where $s\in(1/2,1]$ is such that $\psi\in H^{2+s}(\Omega)\cap X$ (cf. Theorem 2.2) and $\mathcal{G}$ is a suitable function independent of h.

Proof. Let $\psi_I\in X_h$ be the interpolant of ψ, such that Proposition 4.2 holds true. We set $w_h:=\psi_h-\psi_I$. Thus,

$$\|\psi-\psi_h\|_X \le \|\psi-\psi_I\|_X+\|w_h\|_X. \tag{4.5}$$

The bound of first term on the right hand side above follows from Proposition 4.2. Thus, we bound the second term. Thank to properties (3.20), (3.22) and (3.22), we have that

$$\begin{aligned}\mathrm{Re}^{-1}\alpha_1\|w_h\|_X^2 &\le \mathrm{Re}^{-1}A^h(w_h,w_h)=\mathrm{Re}^{-1}A^h(\psi_h,w_h)-\mathrm{Re}^{-1}A^h(\psi_I,w_h)\\ &=\mathrm{Re}^{-1}A^h(\psi_h,w_h)+B^h(\psi_h;w_h,w_h)-\mathrm{Ro}^{-1}C^h_{\mathrm{skew}}(w_h,w_h)-\mathrm{Re}^{-1}A^h(\psi_I,w_h)\\ &=\left[\mathrm{Re}^{-1}A^h(\psi_h,w_h)+B^h(\psi_h;\psi_h,w_h)-\mathrm{Ro}^{-1}C^h_{\mathrm{skew}}(\psi_h,w_h)\right]\\ &\quad -B^h(\psi_h;\psi_I,w_h)+\mathrm{Ro}^{-1}C^h_{\mathrm{skew}}(\psi_I,w_h)-\mathrm{Re}^{-1}A^h(\psi_I,w_h)\\ &=\mathrm{Ro}^{-1}F^h(w_h)-\mathrm{Re}^{-1}A^h(\psi_I,w_h)-B^h(\psi_h;\psi_I,w_h)+\mathrm{Ro}^{-1}C^h_{\mathrm{skew}}(\psi_I,w_h),\end{aligned}$$

where we have used the definition of the discrete scheme (3.26). Now, adding and subtracting the term $\mathrm{Ro}^{-1}F(w_h)$ on the right hand side above, and using the definition of the continuous problem (cf. (2.8)), we get

$$\begin{aligned}\mathrm{Re}^{-1}\alpha_1\|w_h\|_X^2 &\le \mathrm{Ro}^{-1}\left[F^h(w_h)-F(w_h)\right]+\mathrm{Re}^{-1}\left[A(\psi,w_h)-A^h(\psi_I,w_h)\right]\\ &\quad +\left[B(\psi;\psi,w_h)-B^h(\psi_h;\psi_I,w_h)\right]+\mathrm{Ro}^{-1}\left[C_{\mathrm{skew}}(\psi,w_h)-C^h_{\mathrm{skew}}(\psi_I,w_h)\right]\\ &\le C\,\mathrm{Ro}^{-1}\|F-F^h\|_{X_h'}\|w_h\|_X+\mathrm{Re}^{-1}\left[A(\psi,w_h)-A^h(\psi_I,w_h)\right]\\ &\quad +\left[B(\psi;\psi,w_h)-B^h(\psi_h;\psi_I,w_h)\right]+\mathrm{Ro}^{-1}\left[C_{\mathrm{skew}}(\psi,w_h)-C^h_{\mathrm{skew}}(\psi_I,w_h)\right]\\ &= T_F+T_A+T_B+T_C.\end{aligned} \tag{4.6}$$

Now, we bound each term on the right hand side above. First, the term T_F can be easily bounded by using Proposition 4.3. Then, we estimate the term T_A as follows. Adding and subtracting $\psi_\pi\in\mathcal{P}_2(K)$ such that Proposition 4.1 holds true, and using the consistency of the bilinear form $A^{h,K}(\cdot,\cdot)$ (cf. (3.16)), we have that

$$T_A=\mathrm{Re}^{-1}\sum_{K\in\Omega_h}\left[A^K(\psi-\psi_\pi,w_h)-A^{h,K}(\psi_I-\psi_\pi,w_h)\right]\le C\mathrm{Re}^{-1}h^s\|\psi\|_{2+s,\Omega}\|w_h\|_X, \tag{4.7}$$

where we have used the continuity of the bilinear form $A^{h,K}(\cdot,\cdot)$, Propositions 4.1 and 4.2 and Cauchy-Schwarz inequality. Analogously, the term T_C can be estimated as follows

$$T_C=\mathrm{Ro}^{-1}\sum_{K\in\Omega_h}\left[C^K_{\mathrm{skew}}(\psi-\psi_\pi,w_h)-C^{h,K}_{\mathrm{skew}}(\psi_I-\psi_\pi,w_h)\right]\le C\mathrm{Ro}^{-1}h^s\|\psi\|_{2+s,\Omega}\|w_h\|_X. \tag{4.8}$$

The next step is to bound the term T_B. We proceed as follows

$$\begin{aligned}T_B&=\left[B(\psi;\psi,w_h)-B^h(\psi_h;\psi_h,w_h)\right]+\left[B^h(\psi_h;\psi_h,w_h)-B^h(\psi_h;\psi_I,w_h)\right]\\ &=\left[B(\psi;\psi,w_h)-B^h(\psi_h;\psi_h,w_h)\right]+\left[B^h(\psi_h;w_h,w_h)\right]\\ &=B(\psi;\psi,w_h)-B^h(\psi_h;\psi_h,w_h),\end{aligned} \tag{4.9}$$

where we have used (3.22) to obtain the last equality. Now, we add and subtract the term $B^h(\psi;\psi,w_h)$, then we use Lemmas 4.2 and 4.3 to obtain that

$$\begin{aligned}T_B&=\left[B(\psi;\psi,w_h)-B^h(\psi;\psi,w_h)\right]+\left[B^h(\psi;\psi,w_h)-B^h(\psi_h;\psi_h,w_h)\right]\\ &\le C\,h^s(\|\psi\|_X+\|\psi\|_{1+s,\Omega})\|\psi\|_{2+s,\Omega}\|w_h\|_X+\widehat{C_{B^h}}\left(\|\psi_h\|_X\|w_h\|_X+Ch^s\|\psi\|_{2+s,\Omega}(\|\psi\|_X+\|\psi_h\|_X)\right)\|w_h\|_X,\end{aligned} \tag{4.10}$$

where we have used that $w_h=\psi_h-\psi_I$ and then Proposition 4.2.

Therefore, from (4.6), using (4.7)-(4.10), we obtain

$$\begin{aligned}\mathrm{Re}^{-1}\alpha_1\|w_h\|_X &\le C\,\mathrm{Ro}^{-1}\,h^2\|f\|_{0,\Omega}+C(\mathrm{Re}^{-1}+\mathrm{Ro}^{-1})h^s\|\psi\|_{2+s,\Omega}+C\,h^s(\|\psi\|_X+\|\psi\|_{1+s,\Omega})\|\psi\|_{2+s,\Omega}\\ &\quad +\widehat{C_{B^h}}\|\psi_h\|_X\|w_h\|_X+\widehat{C_{B^h}}\,Ch^s(\|\psi\|_X+\|\psi_h\|_X)\|\psi\|_{2+s,\Omega}.\end{aligned}$$

From the inequality above, we obtain

$$\begin{aligned}\mathrm{Re}^{-1}\alpha_1\left(1-\widehat{C_{B^h}}\mathrm{Re}\alpha_1^{-1}\|\psi_h\|_X\right)\|w_h\|_X &\le C\,\mathrm{Ro}^{-1}h^2\|f\|_{0,\Omega}+C(\mathrm{Re}^{-1}+\mathrm{Ro}^{-1})h^s\|\psi\|_{2+s,\Omega}\\ &\quad +C\,h^s(\|\psi\|_X+\|\psi\|_{1+s,\Omega})\|\psi\|_{2+s,\Omega}+\widehat{C_{B^h}}\,Ch^s(\|\psi\|_X+\|\psi_h\|_X)\|\psi\|_{2+s,\Omega}.\end{aligned} \tag{4.11}$$

Next, from (3.31) and the fact that $\psi_h\in\mathcal{N}_h$, it holds that

$$1-\frac{\widehat{C_{B^h}}\|\psi_h\|_X}{\mathrm{Re}^{-1}\alpha_1}\ge 1-\frac{\widehat{C_{B^h}}\,C_1\,\mathrm{Re}^2\,\mathrm{Ro}^{-1}\|f\|_{0,\Omega}}{\alpha_1^2}=1-\lambda_h>0. \tag{4.12}$$

Therefore, from (4.11), (4.12) and Theorem 3.1, we get

$$\begin{aligned}\|w_h\|_X &\le \frac{C\,\mathrm{Re}\,\mathrm{Ro}^{-1}\,h^2\,\|f\|_{0,\Omega}}{\alpha_1\,(1-\lambda_h)}+\frac{C\,\mathrm{Re}\,(\mathrm{Re}^{-1}+\mathrm{Ro}^{-1})h^s}{\alpha_1\,(1-\lambda_h)}\|\psi\|_{2+s,\Omega}\\ &\quad +\frac{C\,\mathrm{Re}\,h^s}{\alpha_1\,(1-\lambda_h)}(\|\psi\|_X+\|\psi\|_{1+s,\Omega})\|\psi\|_{2+s,\Omega}+\frac{\widehat{C_{B^h}}\,C\,\mathrm{Re}\,h^s}{\alpha_1\,(1-\lambda_h)}(\|\psi\|_X+\|\psi_h\|_X)\|\psi\|_{2+s,\Omega}\\ &\le C\,h^s\mathcal{G}(f;\mathrm{Re},\mathrm{Ro},\lambda,\lambda_h),\end{aligned} \tag{4.13}$$

where we have also used Theorem 2.2. Finally, the proof follows from (4.5), (4.13) and Proposition 4.2. □

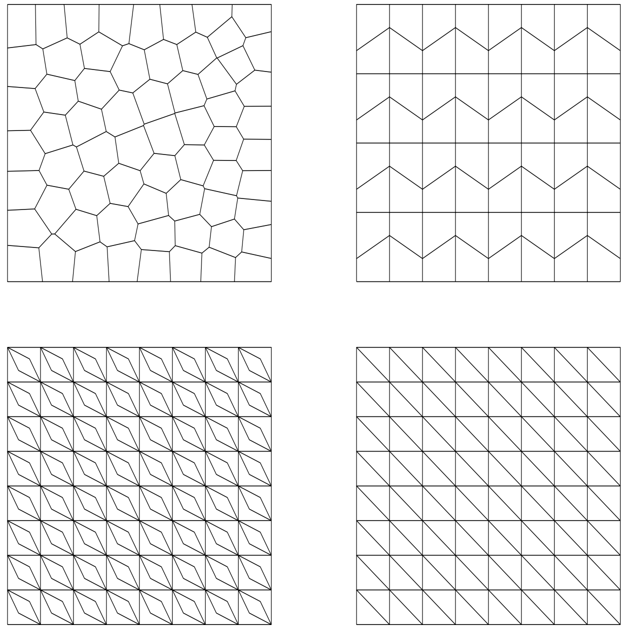

Fig. 1. Sample meshes. Ω_h^1 (top left), Ω_h^2 (top right), Ω_h^3 (bottom left) and Ω_h^4 (bottom right).

5. Numerical results

In this section, we present four numerical experiments, to test the behavior of the proposed VEM discretization (3.26) and in order to verify the theoretical results established in Section 4.

We have tested the virtual scheme by using different families of polygonal meshes (cf. Fig. 1). For reasons of brevity, we do not report the results obtained with all meshes for all test problems. The non reported results are in accordance with the ones shown.

- Ω_h^1: Sequence of CVT (Centroidal Voronoi Tessellation);
- Ω_h^2: Trapezoidal meshes;
- Ω_h^3: Distorted concave rhombic quadrilaterals;
- Ω_h^4: Uniform triangular meshes.

In order to test the convergence of the proposed scheme, we introduce the following computable quantities:

$$\mathtt{e}_i(\psi) := |\psi - \Pi_K^{2,\mathrm{D}} \psi_h|_{i,h}, \quad i = 0, 1, 2.$$

We will compute experimental rates of convergence for each individual error as follows:

$$\mathtt{r}_i(\psi) := \frac{\log(\mathtt{e}_i(\psi)/\mathtt{e}_i'(\psi))}{\log(h/h')}, \quad i = 0, 1, 2,$$

where h, h' denote two consecutive mesh sizes with their respective errors $\mathtt{e}_i$ and $\mathtt{e}_i'$.

For each test to solve the resulting nonlinear system, we used the Newton method with maximum 10 iterations, a tolerance Tol= $1\mathtt{e}-8$ and we take $\psi_h^0 = 0$ as an initial guess; moreover, we have taken the Reynolds number as $\mathrm{Re} = 1.667$ and the Rossby number as $\mathrm{Ro} = 1\mathtt{e}-4$ (see [27]). Finally, we consider $\Omega := (0,1)^2$ as computational domain in the first three examples and an L-shaped domain in the last example.

5.1. Test 1: smooth solution

In this numerical test, we take the load term in such a way that the analytical solution of the quasi-geostrophic equations (2.1) is given by:

$$\psi(x,y) := \frac{1}{\pi^2} \sin^2(\pi x) \sin^2(\pi y) e^{x^2+y^2}.$$

We report in Table 1 the convergence history of our virtual scheme on the meshes Ω_h^1. The table includes the number of degrees of freedom (dofs), the discrete errors $\mathtt{e}_i(\psi)$, the convergence rates $\mathtt{r}_i(\psi)$ for $i = 0, 1, 2$, and the number of iterations (iter) used by the Newton method to achieve tolerance at each level of refinement.

We observe that the asymptotic $\mathcal{O}(h)$ decay of the discrete error $\mathtt{e}_2(\psi)$ observed for the stream-function confirms the optimal convergence predicted by Theorem 4.1. It can be also seen that the errors $\mathtt{e}_0(\psi)$ and $\mathtt{e}_1(\psi)$ decay much faster. However, we have not proved the higher order in these cases. The table also shows that a maximum of four iterations are required for the Newton method.

Sample approximate solutions generated with the virtual method on a coarse mesh are portrayed in Fig. 2.

Table 1
Test 1. Errors and experimental rates for the stream-function ψ_h, using the meshes Ω_h^1.

dofs	h	$\mathrm{e}_0(\psi)$	$\mathrm{r}_0(\psi)$	$\mathrm{e}_1(\psi)$	$\mathrm{r}_1(\psi)$	$\mathrm{e}_2(\psi)$	$\mathrm{r}_2(\psi)$	iter
294	1/8	4.214341e-2	—	1.338770e-1	—	3.676844e-1	—	3
1371	1/16	1.100219e-2	1.937	4.993576e-2	1.422	1.924777e-1	0.933	3
5796	1/32	2.329921e-3	2.239	1.229111e-2	2.022	9.401329e-2	1.033	3
23874	1/64	5.576055e-4	2.062	3.109190e-3	1.983	4.633333e-2	1.020	3
96855	1/128	1.089853e-4	2.355	7.895256e-4	1.977	2.308295e-2	1.005	3

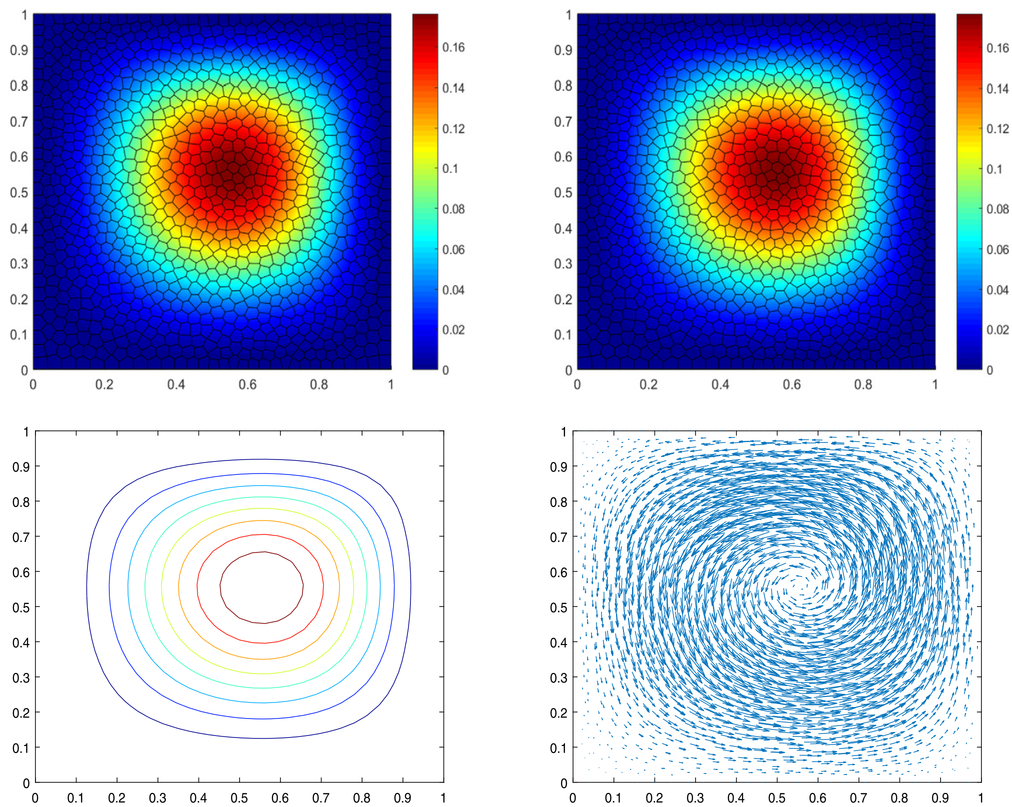

Fig. 2. Test 1. Exact and approximate solutions ψ and ψ_h, the streamlines of ψ_h and the velocity field $\boldsymbol{u}_h := \mathbf{curl}\,\psi_h$ (top left, top right, bottom left, bottom right, respectively), using the VEM method (3.26) with Ω_h^1, $h = 1/32$.

Table 2
Test 2. Errors and experimental rates for the stream-function ψ_h, using the meshes Ω_h^2.

dofs	h	$\mathrm{e}_0(\psi)$	$\mathrm{r}_0(\psi)$	$\mathrm{e}_1(\psi)$	$\mathrm{r}_1(\psi)$	$\mathrm{e}_2(\psi)$	$\mathrm{r}_2(\psi)$	iter
147	1/8	7.600646e-5	—	1.549666e-3	—	2.834095e-2	—	3
675	1/16	1.616079e-5	2.233	4.688010e-4	1.724	1.390167e-2	1.027	2
2883	1/32	2.976015e-6	2.441	1.110449e-4	2.077	7.254667e-3	0.938	2
11907	1/64	6.202604e-7	2.262	2.706962e-5	2.036	3.804474e-3	0.931	2
48387	1/128	1.451048e-7	2.095	6.730940e-6	2.007	1.938996e-3	0.972	3

5.2. Test 2: solution with western boundary layer

In this numerical example, we solve the quasi-geostrophic equations (2.1) by taking the load term in such a way that the analytical solution is given by:

$$\psi(x,y) = \frac{1}{(20\pi)^2}\left((1-x)\left(1-e^{-20x}\right)\sin(\pi y)\right)^2.$$

We observe that in this case the solution has a boundary layer on the left hand side.

In Table 2 we report the convergence history of our virtual scheme on the meshes Ω_h^2. The table includes the number of degrees of freedom (dofs), the discrete errors $\mathrm{e}_i(\psi)$, and the convergence rates $\mathrm{r}_i(\psi)$ for $i = 0, 1, 2$. Once again, the expected order of convergence for the discrete errors $\mathrm{e}_2(\psi)$ is reached.

In addition, in Fig. 3 we display the stream-function (exact and numerical solution) and the approximate velocity field.

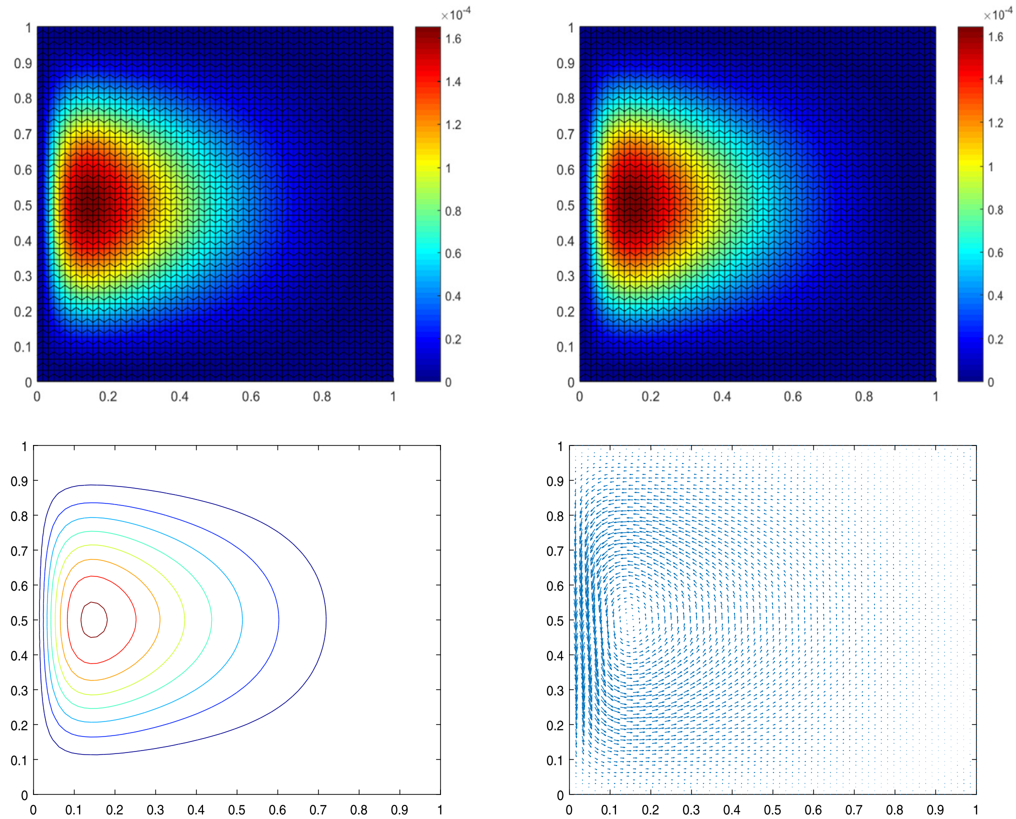

Fig. 3. Test 2. Exact and approximate solutions ψ, ψ_h, the streamlines of ψ_h and the velocity field $\boldsymbol{u}_h := \mathbf{curl}\,\psi_h$ and (top left, top right, bottom left, bottom right, respectively) using the VEM method (3.26) with Ω_h^2, $h = 1/64$.

Table 3
Test 3. Errors and experimental rates for the stream-function ψ_h, using the meshes Ω_h^3.

dofs	h	$\mathrm{e}_0(\psi)$	$\mathrm{r}_0(\psi)$	$\mathrm{e}_1(\psi)$	$\mathrm{r}_1(\psi)$	$\mathrm{e}_2(\psi)$	$\mathrm{r}_2(\psi)$	iter
123	1/4	1.153577e-2	—	2.116982e-1	—	4.17475e+0	—	4
531	1/8	9.705065e-3	0.249	1.328881e-1	0.671	3.21654e+0	0.376	3
2211	1/16	2.444361e-3	1.989	4.017754e-2	1.725	1.72708e+0	0.897	3
9027	1/32	4.937103e-4	2.307	9.985092e-3	2.008	8.549397e-1	1.014	4
36483	1/64	1.118995e-4	2.141	2.479913e-3	2.009	4.275213e-1	0.999	4

5.3. Test 3: solution with vortex in the top-right corner of the domain

In this numerical example, we solve the quasi-geostrophic equations (2.1) by taking the load term in such a way that the analytical solution is given by:

$$\psi(x, y) = \frac{1}{4\pi^2}\left(1 - \cos\left(\frac{2\pi(e^{R_1 x} - 1)}{e^{R_1} - 1}\right)\right)\left(1 - \cos\left(\frac{2\pi(e^{R_2 y} - 1)}{e^{R_2} - 1}\right)\right).$$

In this experiment it is expected to observe a counter-clockwise rotating vortex with center (x_c, y_c) which depends on the values of R_1 and R_2. The coordinates of the center of the vortex are given by:

$$x_c = \frac{1}{R_1}\log\left(\frac{e^{R_1} + 1}{2}\right) \qquad y_c = \frac{1}{R_2}\log\left(\frac{e^{R_2} + 1}{2}\right).$$

In particular, we have chosen $R_1 = R_2 = 4$, then the center of the vortex is located at the top-right corner of the domain. More precisely, $(x_c, y_c) \approx (0.83125, 0.83125)$.

We proceed to study the accuracy of our VEM scheme by solving the discrete problem on a sequence of polygonal meshes Ω_h^3. Once again, we compute the discrete errors $\mathrm{e}_i(\psi)$ for $i = 0, 1, 2$. The error history is collected in Table 3, which indicates that the scheme, as predicted by the theory, converges with an $\mathcal{O}(h)$ in the discrete error $\mathrm{e}_2(\psi)$. The table also shows that a maximum of four iterations are required for the Newton method.

In Fig. 4 we display the stream-function (exact and numerical solution) and the approximate velocity field.

5.4. Test 4: L-shaped domain

Finally, we solve the quasi-geostrophic equations (2.1) on an L-shape domain: $\Omega := (-1, 1)^2 \setminus ([0, 1) \times (-1, 0])$. We take the right hand side term and non-homogeneous Dirichlet boundary conditions in such a way that the exact solution in polar coordinates is given by

$$\psi(r, \theta) = r^{5/3}\sin\left(\frac{5}{3}\theta\right).$$

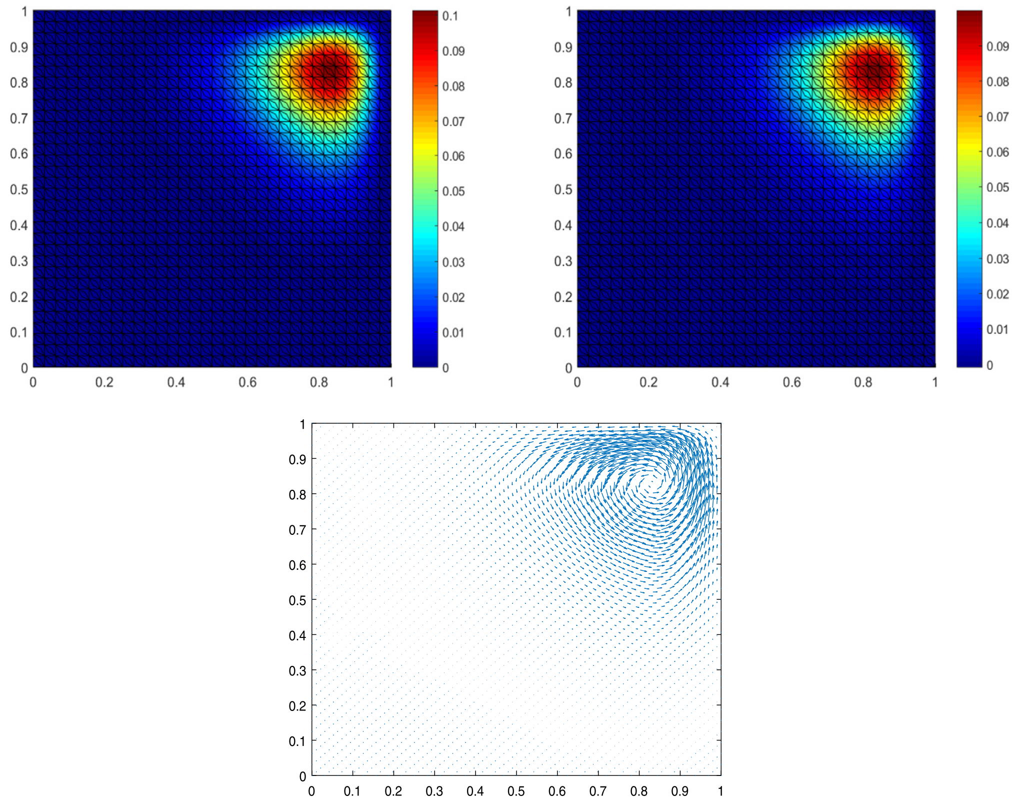

Fig. 4. Test 3. Exact and approximate solutions ψ, ψ_h and the velocity field $\boldsymbol{u}_h := \mathbf{curl}\,\psi_h$ (top left, top right and bottom, respectively) using the VEM method (3.26) with Ω_h^3, $h = 1/32$.

Table 4
Test 4. Errors and experimental rates for the stream-function ψ_h, using the meshes Ω_h^4.

dofs	h	$\mathrm{e}_0(\psi)$	$\mathrm{r}_0(\psi)$	$\mathrm{e}_1(\psi)$	$\mathrm{r}_1(\psi)$	$\mathrm{e}_2(\psi)$	$\mathrm{r}_2(\psi)$	iter
483	1/8	2.985997e-4	—	6.677776e-3	—	2.614276e-1	—	4
2115	1/16	1.448822e-4	1.043	2.446762e-3	1.448	1.643765e-1	0.669	4
8835	1/32	6.100395e-5	1.247	9.069247e-4	1.431	1.040009e-1	0.660	4
36099	1/64	2.538614e-5	1.264	3.411994e-4	1.410	6.577727e-2	0.660	4
145923	1/128	1.063002e-5	1.255	1.316359e-4	1.374	4.155790e-2	0.662	4

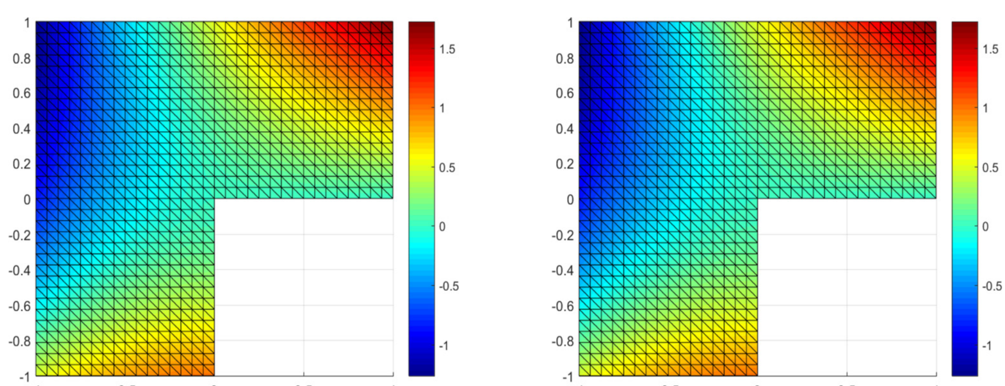

Fig. 5. Test 4. Exact and approximate solutions ψ, ψ_h (left and right, respectively) using the VEM method (3.26) with Ω_h^4, $h = 1/16$.

The analytical solution contains a singularity at the re-entrant corner of Ω; here, we have $\psi \in H^{8/3-\varepsilon}(\Omega)$ for all $\varepsilon > 0$.

Table 4 shows the errors and experimental convergence rates of our virtual scheme on the meshes Ω_h^4. Since the analytical solution is singular, we are not going to obtain linear (in H^2) and quadratic (in H^1 and L^2) order of convergences as in the previous examples. More precisely, according to the regularity of ψ, we expect an order of convergence in H^2 as $\mathcal{O}(h^{2/3})$.

It can be seen from Table 4 that the expected order of convergence for the discrete errors $\mathrm{e}_2(\psi)$ is obtained. We also observe that the errors $\mathrm{e}_0(\psi)$ and $\mathrm{e}_1(\psi)$ decay much faster.

Finally, Fig. 5 shows the stream-function (exact and numerical solution).

Acknowledgements

The first author was partially supported by the National Agency for Research and Development, ANID-Chile through FONDECYT project 1180913 and by project AFB170001 of the PIA Program: Concurso Apoyo a Centros Científicos y Tecnológicos de Excelencia con Financiamiento Basal. The second author was partially supported by the National Agency for Research and Development, ANID-Chile through Scholarship Program, Doctorado Becas Chile 2020, 21201910.

References

[1] R.A. Adams, J.J.F. Fournier, Sobolev Spaces, 2nd ed., Academic Press, Amsterdam, 2003.
[2] I. Al Balushi, W. Jiang, G. Tsogtgerel, T.Y. Kim, A posteriori analysis of a B-spline based finite-element method for the stationary quasi-geostrophic equations of the ocean, Comput. Methods Appl. Mech. Eng. 371 (2020) 113317.
[3] P.F. Antonietti, L. Beirão da Veiga, D. Mora, M. Verani, A stream virtual element formulation of the Stokes problem on polygonal meshes, SIAM J. Numer. Anal. 52 (2014) 386–404.
[4] P.F. Antonietti, L. Beirão da Veiga, S. Scacchi, M. Verani, A C^1 virtual element method for the Cahn–Hilliard equation with polygonal meshes, SIAM J. Numer. Anal. 54 (2016) 36–56.
[5] L. Beirão da Veiga, F. Brezzi, A. Cangiani, G. Manzini, L.D. Marini, A. Russo, Basic principles of virtual element methods, Math. Models Methods Appl. Sci. 23 (2013) 199–214.
[6] L. Beirão da Veiga, F. Dassi, A. Russo, A C^1 virtual element method on polyhedral meshes, Comput. Math. Appl. 79 (7) (2020) 1936–1955.
[7] L. Beirão da Veiga, C. Lovadina, G. Vacca, Divergence free virtual elements for the Stokes problem on polygonal meshes, ESAIM: Math. Model. Numer. Anal. 51 (2017) 509–535.
[8] L. Beirão da Veiga, C. Lovadina, G. Vacca, Virtual elements for the Navier-Stokes problem on polygonal meshes, SIAM J. Numer. Anal. 56 (3) (2018) 1210–1242.
[9] L. Beirão da Veiga, D. Mora, G. Rivera, Virtual elements for a shear-deflection formulation of Reissner-Mindlin plates, Math. Comput. 88 (2019) 149–178.
[10] L. Beirão da Veiga, D. Mora, G. Vacca, The Stokes complex for virtual elements with application to Navier-Stokes flows, J. Sci. Comput. 81 (2) (2019) 990–1018.
[11] H. Blum, R. Rannacher, On the boundary value problem of the biharmonic operator on domains with angular corners, Math. Methods Appl. Sci. 2 (4) (1980) 556–581.
[12] S.C. Brenner, R.L. Scott, The Mathematical Theory of Finite Element Methods, Springer, New York, 2008.
[13] F. Brezzi, L.D. Marini, Virtual elements for plate bending problems, Comput. Methods Appl. Mech. Eng. 253 (2013) 455–462.
[14] E. Cáceres, G.N. Gatica, A mixed virtual element method for the pseudostress-velocity formulation of the Stokes problem, IMA J. Numer. Anal. 37 (2017) 296–331.
[15] A. Cangiani, V. Gyrya, G. Manzini, The nonconforming virtual element method for the Stokes equations, SIAM J. Numer. Anal. 54 (6) (2016) 3411–3435.
[16] J.M. Cascón, G.C. Garcia, R. Rodríguez, A priori and a posteriori error analysis for a large-scale ocean circulation finite element model, Comput. Methods Appl. Mech. Eng. 192 (2003) 5305–5327.
[17] M. Cayco, R.A. Nicolaides, Finite element technique for optimal pressure recovery from stream function formulation of viscous flows, Math. Comput. 46 (174) (1986) 371–377.
[18] M. Cayco, R.A. Nicolaides, Analysis of nonconforming stream function and pressure finite element spaces for the Navier-Stokes equations, Comput. Math. Appl. 18 (8) (1989) 745–760.
[19] A. Chernov, C. Marcati, L. Mascotto, p- and hp-virtual elements for the Stokes problem, Adv. Comput. Math. 47 (2021) 24, 31 pp.
[20] C. Chinosi, L.D. Marini, Virtual element method for fourth order problems: L^2-estimates, Comput. Math. Appl. 72 (8) (2016) 1959–1967.
[21] P.G. Ciarlet, The Finite Element Method for Elliptic Problems, SIAM, 2002.
[22] P.G. Ciarlet, Linear and Nonlinear Functional Analysis with Applications, SIAM, 2013.
[23] F. Dassi, G. Vacca, Bricks for the mixed high-order virtual element method: projectors and differential operators, Appl. Numer. Math. 155 (2020) 140–159.
[24] F. Fairag, A two-level finite-element discretization of the stream function form of the Navier-Stokes equations, Comput. Math. Appl. 36 (1998) 117–127.
[25] D. Fishelov, M. Ben-Artzi, J.-P. Croisille, Recent developments in the pure streamfunction formulation of the Navier–Stokes system, J. Sci. Comput. 45 (2010) 238–258.
[26] G. Fix, Finite element models for ocean circulation problems, SIAM J. Appl. Math. 29 (1975) 371–387.
[27] E.L. Foster, T. Iliescu, Z. Wang, A finite element discretization of the stream function formulation of the stationary quasi-geostrophic equations of the ocean, Comput. Methods Appl. Mech. Eng. 261/262 (2) (2013) 105–117.
[28] E.L. Foster, T. Iliescu, D. Wells, A conforming finite element discretization of the streamfunction form of the unsteady quasi-geostrophic equations, Int. J. Numer. Anal. Model. 13 (6) (2016) 951–968.
[29] G.N. Gatica, M. Munar, F. Sequeira, A mixed virtual element method for the Navier-Stokes equations, Math. Models Methods Appl. Sci. 28 (14) (2018) 2719–2762.
[30] V. Girault, P.A. Raviart, Finite Element Methods for Navier-Stokes Equations, Springer-Verlag, Berlin, 1986.
[31] R.J. Greatbatch, B.T. Nadiga, Four-gyre circulation in a barotropic model with double-gyre wind forcing, J. Phys. Oceanogr. 30 (2000) 1461–1471.
[32] D.B. Haidvogel, A.R. Robinson, E.E. Schulman, The accuracy, efficiency, and stability of three numerical models with application to open ocean problems, J. Comput. Phys. 34 (1980) 1–53.
[33] D. Kim, T.Y. Kim, E.J. Park, D.W. Shin, Error estimates of B-spline based finite-element methods for the stationary quasi-geostrophic equations of the ocean, Comput. Methods Appl. Mech. Eng. 353 (2018) 255–272.
[34] D. Kim, A.K. Pani, E.J. Park, Morley finite element methods for the stationary quasi-geostrophic equation, Comput. Methods Appl. Mech. Eng. 375 (2021) 113639, 21 pp.
[35] T.Y. Kim, E.J. Park, D.W. Shin, A C^0-discontinuous Galerkin method for the stationary quasi-geostrophic equations of the ocean, Comput. Methods Appl. Mech. Eng. 300 (2015) 225–244.
[36] T.Y. Kim, T. Iliescu, E. Fried, B-spline based finite-element method for the stationary quasi-geostrophic equations of the ocean, Comput. Methods Appl. Mech. Eng. 286 (2015) 168–191.
[37] X. Liu, R. Li, Z. Chen, A virtual element method for the coupled Stokes-Darcy problem with the Beaver-Joseph-Saffman interface condition, Calcolo 56 (4) (2019) 48, 28 pp.
[38] X. Liu, Z. Chen, The nonconforming virtual element method for the Navier-Stokes equations, Adv. Comput. Math. 45 (1) (2019) 51–74.
[39] A. Majda, Introduction to PDEs and Waves for the Atmosphere and Ocean, American Mathematical Society, New York, 2003.
[40] A. Majda, X. Wang, Nonlinear Dynamics and Statistical Theories for Basic Geophysical Flows, Cambridge University Press, 2006.
[41] J. McWilliams, Fundamentals of Geophysical Fluid Dynamics, Cambridge University Press, 2006.
[42] T.T. Medjo, Numerical simulations of a two-layer quasi-geostrophic equation of the ocean, SIAM J. Numer. Anal. 37 (2000) 2005–2022.
[43] P.G. Myers, A.J. Weaver, A diagnostic barotropic finite-element ocean circulation model, J. Atmos. Ocean. Technol. 12 (1995) 511–526.
[44] D. Mora, G. Rivera, I. Velásquez, A virtual element method for the vibration problem of Kirchhoff plates, ESAIM: Math. Model. Numer. Anal. 52 (2018) 1437–1456.
[45] J. Pedlosky, Geophysical Fluid Dynamics, Springer, 1987.
[46] G.K. Vallis, Atmosphere and Ocean Fluid Dynamics: Fundamentals and Large-Scale Circulation, Cambridge University Press, 2006.
[47] G. Vacca, An H^1-conforming virtual element for Darcy and Brinkman equations, Math. Models Methods Appl. Sci. 28 (2018) 159–194.
[48] J. Zhao, B. Zhang, S. Mao, S. Chen, The divergence-free nonconforming virtual element for the Stokes problem, SIAM J. Numer. Anal. 57 (6) (2019) 2730–2759.